The influence of prolonged instrument manipulation on gas leakage through trocars

An experimental study

M. van Duijn
Supervisors: Dr. Ir. T. Horeman, Ir. D. Robertson
Graduation date: 17-11-2022

TU Delft Delft University of Technology

The influence of prolonged instrument manipulation on gas leakage through trocars: An experimental study

Matthijs van Duijn
Student number 5173922
BioMedical Engineering
Delft University of Technology

Abstract
Background: During laparoscopic surgery gas could leak from the intra-abdominal cavity into the operating theatre. Medical staff could therefore be exposed to hazardous substances present in leaked gas. Although previous studies have shown that leakage through trocars is a contributing factor, trocar performance over time regarding gas leakage remains unclear. Therefore this study investigates the influence of prolonged instrument manipulation on gas leakage through trocars.
Methods: An experimental setup was developed to allow for instrument manipulation under loading. The trocar was mounted to a custom airtight container. The container was insufflated with CO_2 to a pressure of 15 mmHg, similar to clinical practice. A linear stage was used for prolonged instrument manipulation, and a fixed load was applied to the trocar. Before, after, and during instrument manipulation leakage was measured in 25 trocars with diameters ranging from 10-15 mm.
Results: Leakage rates per trocar varied between 0.0 (0.0-0.0) L/min and 5.58 (5.10-6.49) L/min after instrument manipulation. Two trocars showed visible damage to the trocar valve after manipulation. No statistical difference was found between leakage rates before and after prolonged manipulation in both static and dynamic measurements.
Conclusion: Prolonged instrument manipulation did not influence gas leakage rates through trocars. Nevertheless, gas leakage through trocars occurs and is caused by different trocar-specific mechanisms.

1 Introduction

Over the years, many technical advancements have been made in surgery. One of the most impactful innovations was the introduction of minimally invasive surgery (MIS) [1]. During MIS, small incisions are made to accommodate long instruments and an endoscopic camera. MIS improves important outcomes in many procedures compared to open surgery, such as postoperative pain, scarring, infections, and length of postoperative stay [2–5]. In MIS, the surgical site is inflated with carbon dioxide (CO_2) to create sufficient space for tissue manipulation. An insufflator is used to inflate CO_2 to differential pressures commonly between 12-16 mmHg [6,7]. Trocars act as the access port between the exterior and intra-abdominal environments. Valves inside the trocar prevent CO_2 from escaping the intra-abdominal cavity. Despite the presence of trocar valves, recent research shows that gas leakage could still occur [8, 9].

Leaked gas could contain carcinogenic particles, exposing operating personnel [10–14]. In addition, aerosols generated during MIS can carry viral material. Aerosolized human papillomavirus (HPV) and hepatitis B virus have already been detected in surgical smoke [15]. Therefore concerns about SARS-CoV-2 virus transmission during MIS were raised during the COVID-19 pandemic. No cases of intraoperative transmission have yet been reported. However, SARS-CoV-2 is known to be viable in aerosols for multiple hours, creating a theoretical risk of transmission [16]. Surgeons indicated they were worried about contracting COVID-19 during surgery, stressing concerns in clinical practice [17]. Therefore there is a need for research clarifying the safety of MIS with regard to gas leakage.

Previous research addressing gas leakage has mainly focused on investigating the composition of intra-abdominal gas and its harmful effects [10, 18–20]. Studies quantifying gas leakage during different clinical scenarios are still scarce [8, 21, 22]. Three different leakage mechanisms have been described: leakage through the instrument shaft, between the trocar and the incision, and through the trocar [8]. Leakage through the instrument's shaft depends on the individual instrument design and can be considered constant during surgery. Leakage between the trocar and the incision is associated with incision size, abdominal wall composition, and entry technique, making leakage quantities partly subject to the personal skill level of the surgeon. Finally, leakage through trocars is influenced by the interaction between the trocar and the instrument [9]. Previous studies showed that especially trocars with diameters of 10 mm and above showed significant gas leakage [8, 9, 22]. However, no studies have investigated gas leakage performance of trocars over time during prolonged instrument manipulation. Since such loading is representative of clinical practice, insight into the trocar's performance under these circumstances is paramount in illuminating gas leakage during surgery. Therefore, this study investigates the influence of prolonged instrument manipulation on gas leakage through trocars with diameters of 10 mm and above.

2 Methods

Experimental Setup

After pilot testing, an experimental setup was developed based on predefined requirements to evaluate the research goal (Appendix A). A schematic overview of the experimental setup is presented in Figure 1. A detailed description of the experimental setup is presented in Appendix B.

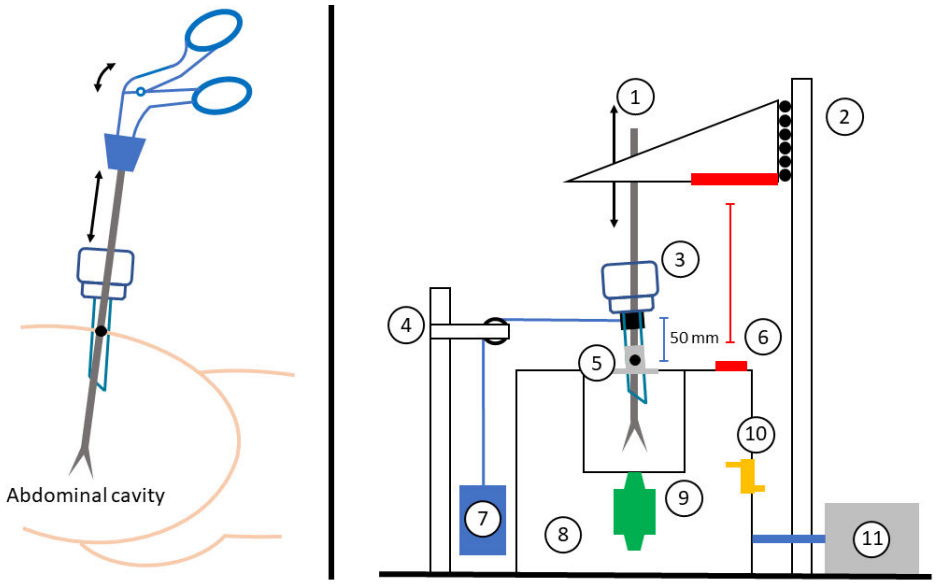

Fig. 1: Laparoscopic surgery (left) and experimental setup (right) 1: Laparoscopic instrument, 2: Linear stage, 3: Trocar, 4: Pulley frame, 5: Trocar Mount, 6: Distance sensor, 7: Weight, 8: Airtight container, 9: Flow sensor, 10: Differential pressure sensor, 11: Insufflator

An airtight, rigid acrylic container (200x200x250 mm) with a wall thickness of 5 mm was designed in SolidWorks (Version 2021 SP3.0, Educational Edition, Dassault Systèmes SolidWorks Corp., Waltham, Massachusetts, USA). A wall thickness of 5 mm was chosen to limit pressure fluctuations due to the deformation of the container during instrument manipulation. Multiple through holes were added to the container to accommodate the trocar, insufflation hose, pressure sensor outlet, and wiring. Through holes were air tightened with custom silicone nozzles. Additionally, two access lids were added to access internal electronics. Acrylic parts were glued together using Acrifix® 1R 0192 (Röhm GmbH, Weiterstadt, Germany). All openings were fastened using M5 nuts and bolts. The setup was mounted to a threaded bottom plate, and custom spacers were developed to ensure proper alignment between components throughout testing.

During laparoscopic surgery, instrument manipulation is a complex combination of axial, pivotal, and radial displacements, causing an altering load to the trocar valves. As a simplification, the instrument was manipulated solely in the axial direction in this study. Simultaneously, a load was applied to the trocar to mimic the interacting force between the instrument and the trocar. The trocar was mounted in the acrylic container using a silicone nozzle with a smaller diameter than the trocar to prevent leakage along the trocar. The trocar's pivot point was fixated, and a second clamp was connected to the trocar 50 mm above the pivot point. The upper clamp was connected to the proximal end of the trocar's shaft. This method allowed for equal loading of all trocars to be tested. A static weight of 1100 grams was attached to the upper clamp using a wire and pulley, resulting in a moment of 0.54 nm. This load is in line with loads applied during laparoscopic surgery [23, 24] (Appendix C). A linear stage (Festo EGSL-BS-55-250-12.7P, Festo, Esslingen am Neckar, Germany) was used for the instrument's axial displacement inside the trocar. The Festo configuration tool was used to preprogram the displacements and velocities. The linear stage executed all displacements of the instrument to ensure equal displacements and velocities for all measurements. Measurements were timed, started, and stopped manually.

During the experiment, the container was insufflated using a Karl Storz (Electronic Endoflator Model 26 4305 20 [25]) insufflator connected to a CO_2 bottle, similar to clinical practice. During surgery, the insufflation hose is connected to a trocar. During this study, the insufflation hose was connected to a dedicated nozzle at the bottom of the container to prevent the insufflation flow from distorting the opposing leakage flow. Figure 2 shows an overview of the final test setup.

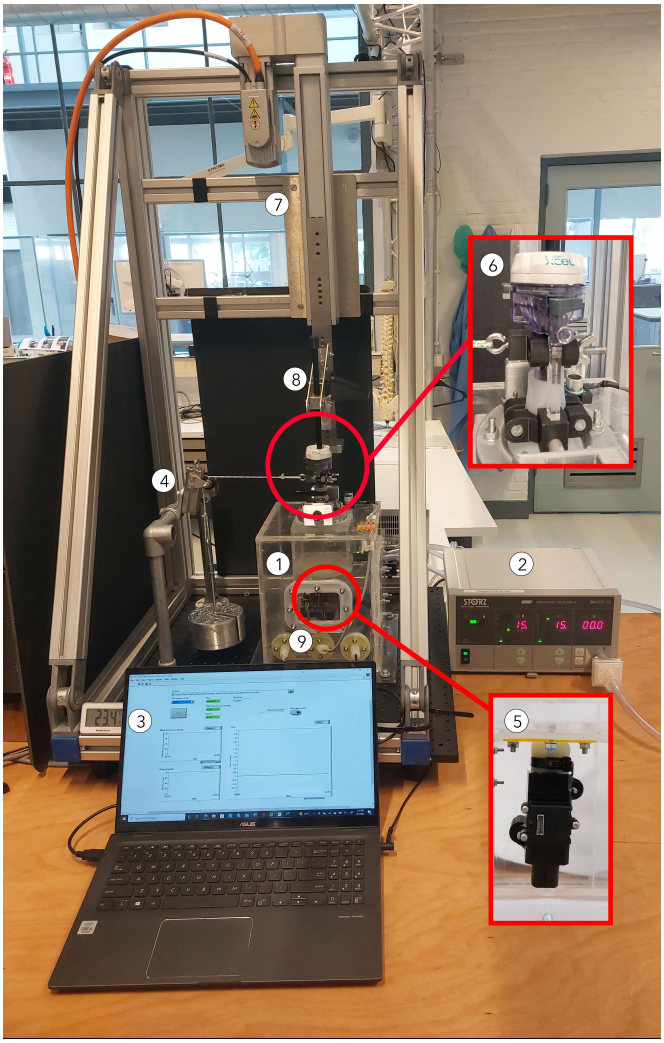

Fig. 2: Overview test setup. 1: Acrylic container, 2: Insufflator, 3: Laptop running LabView, 4: Static load, 5: Flow sensor, 6: Trocar mount, 7: Linear stage, 8: Laparoscopic instrument, 9: Arduino UNO R3 microcontroller

Trocars

Surgeons associated with the European Association for Endoscopic Surgery (EAES) were asked to send in trocars that they would use in

clinical practice. Trocars with a nominal inner diameter of 10 mm or above were included. Both newly sealed disposable, and reusable trocars with new valves were included. All trocars were inspected for defects and categorized prior to testing.

Protocol

Static measurements were taken before (baseline) and after (control) dynamic measurements to evaluate the influence of prolonged trocar loading on gas leakage rates. The dynamic measurements represent prolonged instrument manipulation under loading comparable to clinical practice. In addition, repeated instrument removals and insertions were added to mimic instrument exchanges. During testing the insufflation pressure was set to 15 mmHg with a flow of 15 L/min.

All tests were conducted with a 5 mm (Covidien LigaSure™ Blunt Tip Laparoscopic Sealer) and a 10 mm (Covidien Endo Babcock™) instrument. Certified laparoscopic instruments were used to ensure that the friction between the instrument and the trocar valve was similar to clinical practice. The instrument's handle was removed, and the proximal shaft was capped to prevent leakage through the instrument shaft during measurements. No additional lubrication was added during testing following the instructions for use provided with new trocars.

Before the measurement of every trocar, the container was flushed with 35 liters of CO_2 to ensure saturation with CO_2 (Appendix D). Subsequently, the silicone trocar nozzle was sealed, and the container was pressurized to 15 mmHg to obtain a zero leakage flow measurement for 30 seconds. This measurement was used to calibrate the offset of the flow sensor. Per trocar, a total of 18 measurements were conducted. The order of the measurements was chosen to increase loading severity over time. All measurement steps are described consecutively in Table 1 and visualized in Figure 3.

The test sequence was initiated with the obturator inside the trocar. In clinical practice, the procedure also starts with the obturator inserted during trocar

Table 1: Measurement steps per trocar

Step	Identifier	Action	Instrument	Load	Instrument ⌀ (mm)	Duration (min)
1	**BUO**	Static obturator inserted	Static	Unloaded	-	1
2	**BE5**	Empty trocar	Static	Unloaded	-	1
3	**BU5**	Static instrument inserted	Static	Unloaded	5	1
4	**BL5**	Static instrument inserted	Static	Loaded	5	1
5	**DU5**	Axial instrument manipulation	Dynamic	Unloaded	5	20
6	**DL5**	Axial instrument manipulation	Dynamic	Loaded	5	20
7	**IR5**	Instrument inserted and retracted from trocar	Dynamic	Unloaded	5	18 times
8	**CU5**	Static instrument inserted	Static	Unloaded	5	1
9	**CL5**	Static instrument inserted	Static	Loaded	5	1
10	**MSE***	Empty trocar	Static	Unloaded	-	1
11	**BU10**	Static instrument inserted	Static	Unloaded	10	1
12	**BL10**	Static instrument inserted	Static	Loaded	10	1
13	**DU10**	Axial instrument manipulation	Dynamic	Unloaded	10	20
14	**DL10**	Axial instrument manipulation	Dynamic	Loaded	10	20
15	**IR10**	Instrument inserted and retracted from trocar	Dynamic	Unloaded	10	18 times
16	**CU10**	Static instrument inserted	Static	Unloaded	10	1
17	**CL10**	Static instrument inserted	Static	Loaded	10	1
18	**CE10**	Empty trocar	Static	Unloaded	-	1

* Doubled as the control for 5 mm instrument (CE5) and baseline for 10 mm instrument (BE10)

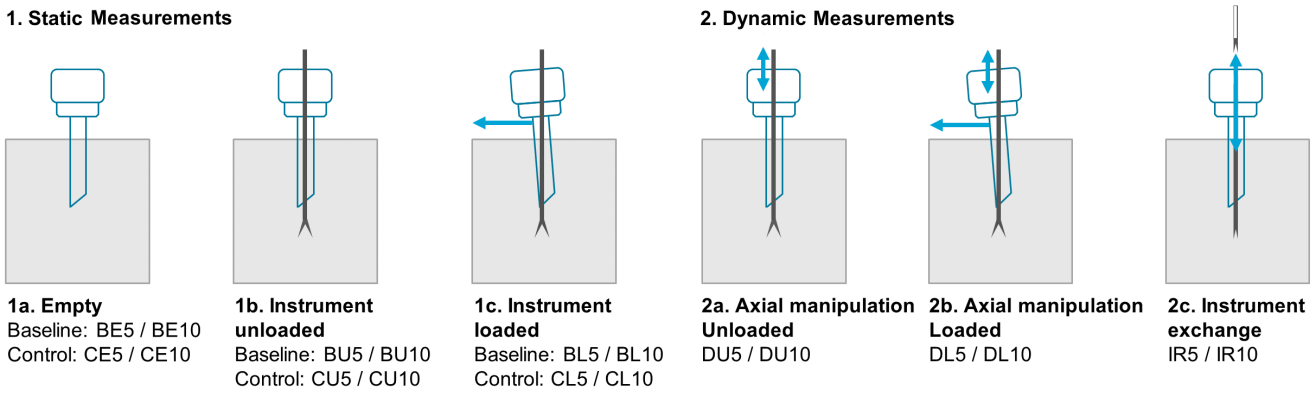

Fig. 3: Schematic overview of measurements

placement. Static measurements included measuring the empty trocar and the trocar with an inserted instrument (Figure 3). The instrument was inserted past all trocar valves with the instrument tip protruding from the cannula. The instrument was then kept static with the linear stage, and leakage was measured for one minute. This measurement was conducted with and without the load applied to the trocar.

Three dynamic measurements applied prolonged loading to the trocar (Figure 3) and were taken between the static baseline and control measurements. The first two measurements included unloaded and loaded axial manipulation for 20 minutes. During manipulation, a stroke length of 30 mm and a velocity of 25 mm/s were used. This velocity is common during instrument manipulation by experts [26]. Additionally, the instrument was inserted past all trocar valves and entirely removed from the trocar 18 times in a row. This value was retrieved by pooling data from multiple trials and calculating the average exchange rate during 40 minutes of surgery [27–37]. The removal and insertion velocity was set to 40 mm/s. The empty trocar control measurements from the 5 mm instrument sequence doubled as the empty trocar baseline measurement for the 10 mm instrument sequence.

All trocar valves were inspected for visual damage after the final measurement. Additional trocar-specific testing was conducted based on observations during testing (e.g. peaks in the flow curve, audible gas leakage, visible valve damage). If leakage was suspected, a soap test was performed to locate the leakage.

Data acquisition

A flow sensor (Honeywell Zephyr, HAFUHH0050L4AXT [38], Honeywell International Inc., Charlotte, North Carolina, USA) was located collinearly to the trocar tip to measure gas leakage. The flow sensor was calibrated using a calibration syringe (Hans Rudolph series 5530, Hans Rudolph inc., Shawnee, Kansas, USA [39]) (Appendix D). The differential pressure between the lab environment and the inside of the container was measured using a pressure sensor (Honeywell ABPMRRN060MGAA5 [40], Honeywell International Inc., Charlotte, North Carolina, USA). The space between the instrument mount and container was measured using an ultrasonic distance sensor (HC-SR04 [41], SparkFun Electronics, Niwot, Colorado, USA) to track instrument displacement during manipulation of the instrument. Sensor data was retrieved with an Arduino Uno R3 [42] microcontroller with a sampling frequency of 40Hz. Flow, pressure, and distance data from the microcontroller were recorded in LabVIEW (Version 18.0f2, National Instruments, Austin, Texas, USA) (Appendix E). A new measurement file was created for every trocar, and individual measurements were stored separately. In addition, CO_2 concentration levels were monitored using a thermal conductivity sensor (Sensirion STC31, Sensirion AG, Stäfa, Switzerland [43]). CO_2 levels (%) were displayed using an Arduino Uno R3. The wiring and programming of both microcontrollers are presented in Appendix F.

Data processing and statistical analysis

For this research, IBM SPSS Statistics (Version 28.0.1.1, IBM, Armonk, New York, USA) was used for statistical analysis. Diadem (Version 22.0.0f8498, National Instruments, Austin, Texas, USA) was used for data processing, and OriginPro (Version 9.8.0.200, OriginLab Corporation, Northampton Massachusetts, USA) was used for visualizations. Test data was evaluated and tested for normality with a Shapiro-Wilk test. If acquired data proved to be normally distributed, leakage values would be reported as means with standard deviations (std.). The difference between the control and baseline measurement will be presented by subtracting the baseline from the control measurement (e.g. CU5-BU5, CL5-BL5, etc.). A Paired Samples T-test would be used to evaluate differences between baseline and control measurements. Differences between leakage at the start and end of a dynamic measurement would also be compared. In case of non-normal distribution, summary values would be reported as medians with interquartile range (IQR), and a Wilcoxon Signed Ranks test would be used for comparisons. The significance level was set to $p < 0.05$. Missing values were excluded from the statistical analysis. This could occur when for example the trocar does not allow for both 5 mm and 10 mm instruments.

3 Results

Included trocars

A total of 25 trocars from six different brands were included in this study. Twelve unique trocar types could be distinguished with diameters ranging from 10-15 mm. Most trocars were disposable trocars (n=22). One reusable trocar type was included. The bottom valve was reusable, while the top valve had to be replaced after usage. This reusable trocar was only compatible with 10 mm instruments. Therefore, 22 trocars were tested with both 5 mm and 10 mm instruments, and three trocars were tested with 10 mm instruments only. None of the trocars showed visible defects before testing. Equal trocar types were grouped together. An overview of all included trocars is presented in Table 2.

Raw data

Figure 4 shows an example of a one-minute unloaded static measurement with a 5 mm instrument. Both the flow and pressure curves are plotted. Two peaks in the flow data occur during insufflation, these peaks correspond to peaks in the pressure curve. In between the peaks, the flow remains steady at around 0.06 L/min.

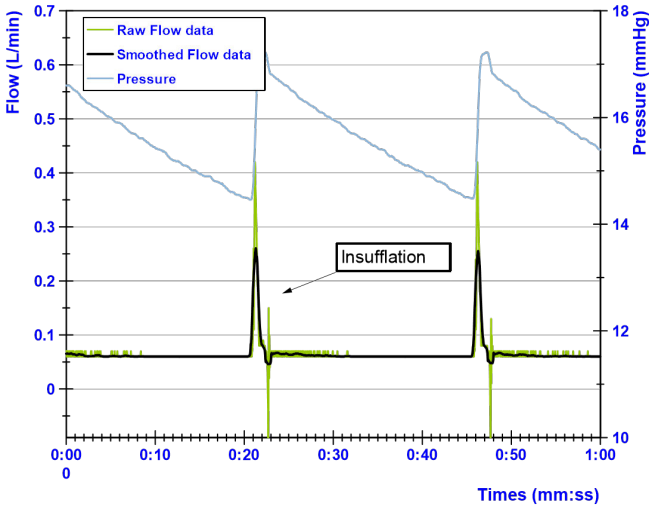

Fig. 4: Example of static flow measurement

Figure 5 shows a short sample of 30 seconds from a 20-minute dynamic unloaded measurement with a 5 mm instrument. The distance curve oscillates corresponding to the up- and downstroke of the instrument. One additional peak around 0.4 L/min occurs during insufflation. Flow data from both static and dynamic measurements were not normally distributed. Therefore, medians (IQR) and non-parametric tests will be used to present results and for further analysis.

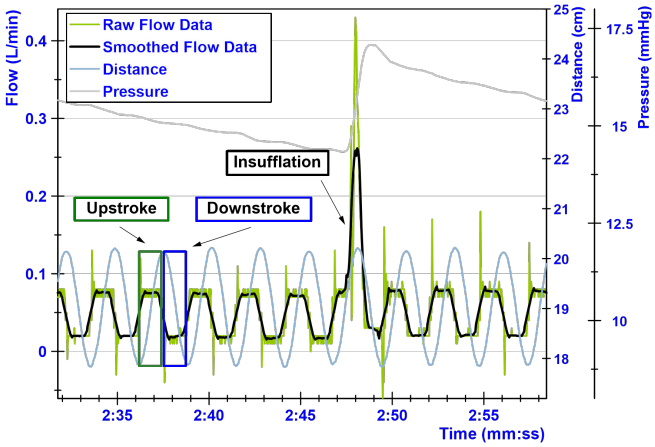

Fig. 5: Example of dynamic flow measurement

Table 2: Overview of included trocars

Label	Group	Brand	Type	Use type	Diameter (mm)	REF
1	1	Sejong Medical	Laport Disposable Trocar System	Disposable	12	T11-1210
2		Sejong Medical	Laport Disposable Trocar System	Disposable	12	T11-1210
3		Sejong Medical	Laport Disposable Trocar System	Disposable	12	T11-1210
4	2	Applied Medical	Kii Fios First Entry	Disposable	12	CFF73
5		Applied Medical	Kii Fios First Entry	Disposable	12	CFF73
6		Applied Medical	Kii Fios First Entry	Disposable	12	CFF73
7	3	Applied Medical	Kii Optical Access System	Disposable	15	C0R37
8		Applied Medical	Kii Optical Access System	Disposable	15	C0R37
9		Applied Medical	Kii Optical Access System	Disposable	15	C0R37
10	4	Covidien	VersaStep Plus	Disposable	12	VS101012P
11		Covidien	VersaStep Plus	Disposable	12	VS101012P
12		Covidien	VersaStep Plus	Disposable	12	VS101012P
13	5	Karl Storz	HICAP with multifunctional valve	Reusable	12	30107
14		Karl Storz	HICAP with multifunctional valve	Reusable	12	30107
15		Karl Storz	HICAP with multifunctional valve	Reusable	12	30107
16	6	Ethicon	Endopath Excel	Disposable	12	B12LT
17		Ethicon	Endopath Excel	Disposable	12	B12LT
18	7	Ethicon	Endopath Excel	Disposable	11	B11LT
19		Ethicon	Endopath Excel	Disposable	11	B11LT
20	8	Ethicon	Endopath Excel	Disposable	12	D12LT
21		Ethicon	Endopath Excel	Disposable	12	D12LT
22	9	Covidien	VersaOne	Disposable	12	NONB12STF
23	10	Covidien	VersaPort Plus V2	Disposable	12	179096PF
24	11	Covidien	Auto Suture	Disposable	10	OMS-T10BT
25	12	Mölnlycke Health Care	Bladeless Dilating Tip Trocar	Disposable	12	899312

Trocar leakage

Median leakage rates after manipulation (control measurement) per trocar are shown in Figure 6. Trocars from group 5 could only be tested with a 10 mm instrument. Therefore only three measurements are presented. Six measurements are presented for all other trocars. From a total of 141 measurements, 132 (93%) had a median leakage < 0.2 L/min. Trocars in group 3 showed a median leakage ranging from 0.30-0.41 L/min for loaded measurements with a 5 mm instrument. Trocar 24 showed leakage of the empty trocar ranging from 0.29-0.36 L/min. Trocars in group 6 showed the highest leakage rates. Trocar 17 had a median leakage of 5.58 (5.10-6.49) L/min and 5.17 (4.94-6.03) L/min for the loaded measurements with 5 mm and 10 mm instruments respectively.

Median leakage during manipulation is presented in Figure 7. Trocars 16 and 17 showed the highest leakage rates during loaded manipulation. For trocar 17 leakage rates were 5.58 (4.94-6.87) L/min and 5.85 (5.05-7.12) L/min for loaded manipulation with a 5 mm and 10 mm instrument respectively.

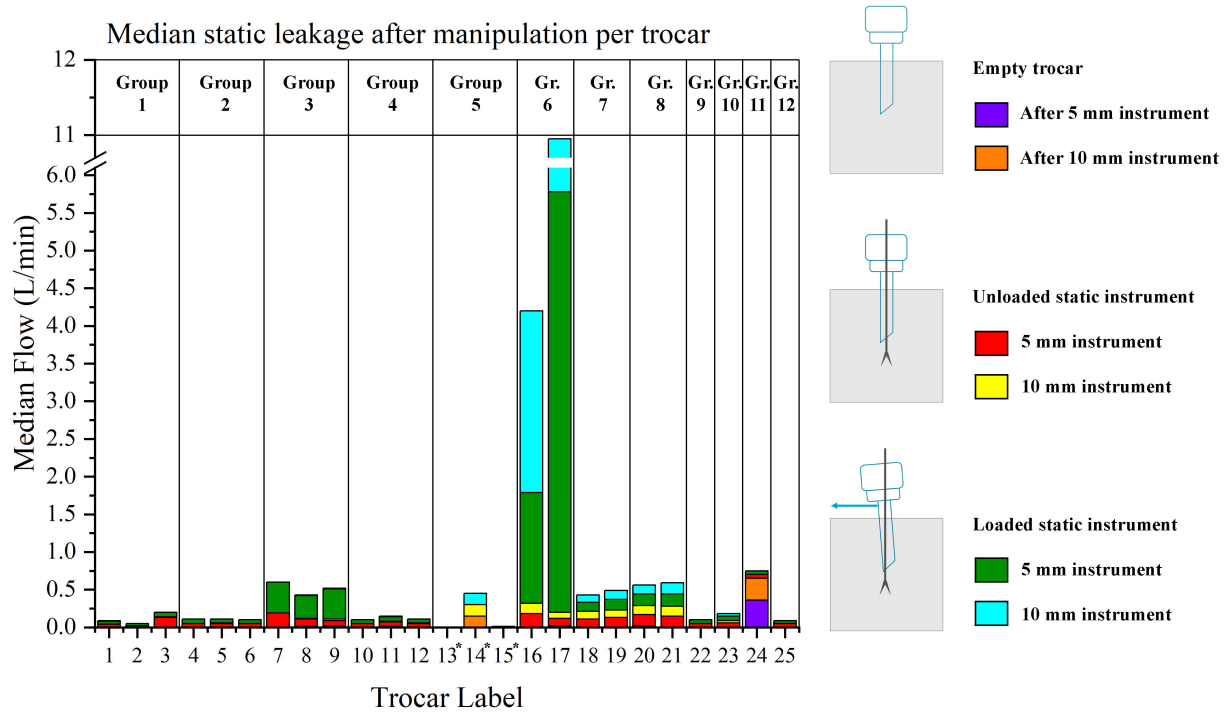

Fig. 6: Median static leakage after manipulation per trocar. *: Trocar was only tested with a 10 mm instrument

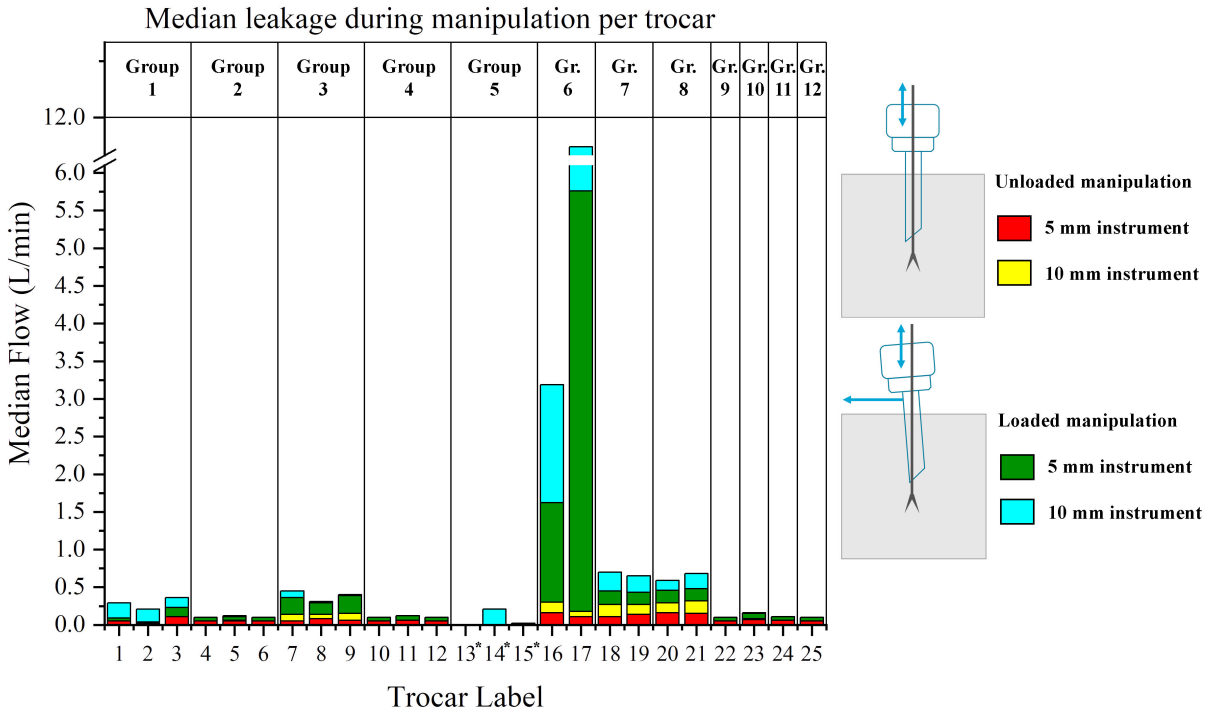

Fig. 7: Median leakage during manipulation per trocar. *: Trocar was only tested with a 10 mm instrument

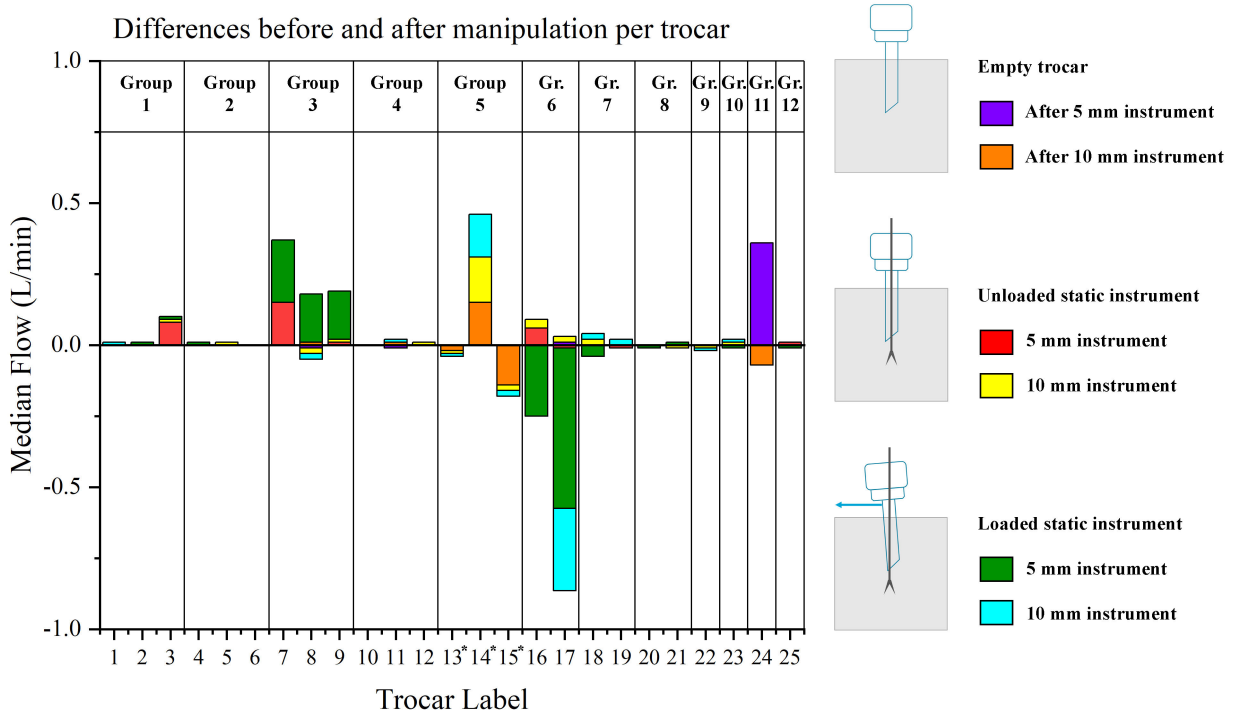

Fig. 8: Median differences before and after manipulation per trocar. Calculated by subtracting the static baseline measurement from the static control measurement. *: Trocar was only tested with a 10 mm instrument.

Figure 8 shows the differences between the static control measurement after manipulation and the static baseline measurement before manipulation. Positive values indicate that median leakage from the control measurement was higher than the baseline measurement. An increase in median leakage larger than 0.1 L/min was seen in trocars 7,8,9,14, and 24. Trocars 7,8,9 were from the same group, and all showed increased median leakage ranging from 0.17-0.22 L/min after manipulation in loaded trocars with a 5 mm instrument inserted. Trocar 14 showed increased median leaking ranging from 0.15-0.16 L/min in all measurements regarding the 10 mm instrument. Lastly, trocar 24 showed an increased median leakage of 0.36 L/min in the empty trocar measurement after manipulation with a 5 mm instrument. Trocars 16 and 17 showed reduced leakage rates ranging from 0.25-0.56 L/min after manipulation in loaded measurements. Trocar 15 showed a reduction of 0.14 L/min in median leakage in the empty trocar after manipulation with a 10 mm instrument.

Table 3 shows the results of the Wilcoxon Signed Ranks Test comparing the median leakage of the control and baseline measurements. The empty trocar (E), unloaded trocar (U), and loaded trocar (L) measurements with a 5 mm and 10 mm instrument were all compared. No statistical difference was found between median leakage rates before and after manipulation with a 5 mm or 10 mm instrument.

Table 3: Comparison of static measurements before and after manipulation[a,b]

	E5	U5	L5	E10	U10	L10
Z	-.378[c]	-1.549[c]	-.036[c]	-.315[d]	-1.157[c]	-.090[c]
Asymp. Sig. (2-tailed)	.705	.121	.972	.752	.247	.928

a. Wilcoxon Signed Ranks Test control versus baseline measurement
b. E5/10: Empty trocar before/after manipulation 5/10 mm instrument
U5/10: inserted 5/10 mm instrument unloaded
L5/10: inserted 5/10 mm instrument loaded
c. Based on negative ranks.
d. Based on positive ranks.

Table 4 shows the results of the Wilcoxon Signed Ranks Test to compare the median leakage rate at the start (t_0: 00:30) versus the end (t_1: 18:30) of a dynamic manipulation measurement. The median was calculated from one minute of flow data. The unloaded manipulation (DU) and loaded manipulation (DL) measurements with 5 mm and 10 mm instruments were included in the comparison. No statistical difference was found between the median leakage at the start and the end of all measurements.

Table 4: Comparison start versus end of dynamic instrument manipulation[a,b]

	DU5	DL5	DU10	DL10
Z	-.832[c]	-.090[d]	-1.301[c]	-.536[c]
Asymp. Sig. (2-tailed)	.405	.928	.193	.592

a. Wilcoxon Signed Ranks Test comparing end versus start dynamic measurements
b. One-minute measurement from start t_0: 00:30 and end: t_1: 18:30
DU5/10 : Dynamic unloaded manipulation with 5/10 mm instrument
DL5/10 : Dynamic loaded manipulation with 5/10 mm instrument
c. Based on negative ranks.
d. Based on positive ranks.

Individual trocars

Of all 25 trocars, two trocars (1, 24) showed visible damage. In trocar 1 the upper trocar valve was clamped between the instrument and the trocar during loaded manipulation with a 5 mm instrument (Figure 9). Subsequently, a tear developed in the trocar valve (Figure 10).

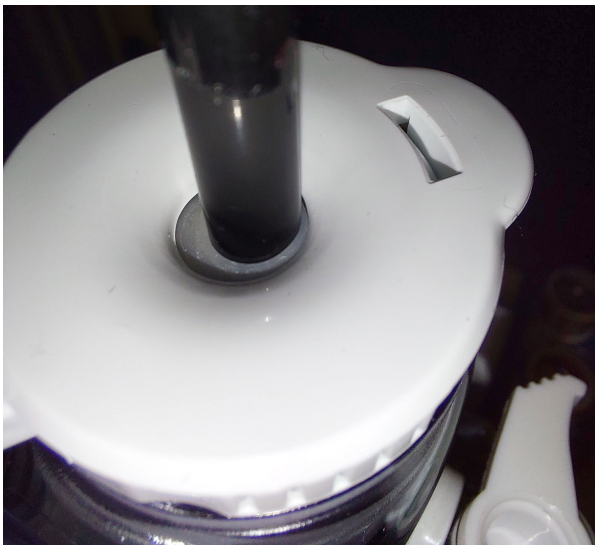

Fig. 9: Trocar valve clamped between instrument and trocar

Fig. 10: Tear in upper trocar valve

Additional testing was performed to evaluate the influence of tear orientation relative to the trocar load. First, the tear was positioned opposite to the load direction, pushing the instrument into the damaged valve (Figure 11, top). Second, the valve was rotated 180 degrees pushing the instrument away from the tear (Figure 11, bottom). In the first test condition, the median leakage was 0.06 (0.05-0.06) L/min, while the median leakage was 1.65 (1.56-1.80) L/min, in the second test condition.

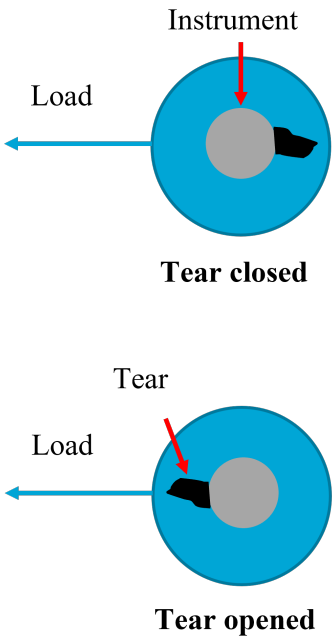

Fig. 11: Tear testing conditions. Top: tear opposite to trocar load. Bottom: tear in line with trocar load.

Trocar 24 showed valve damage to the lower valve after manipulation (Figure 12). The lower valve prevents leakage of the empty trocar. Before valve damage, the empty trocar leakage was 0.0 (0.0 – 0.0) L/min. Repeated measurement with the damaged valve resulted in a median leakage of 0.36 (0.34-0.38) L/min.

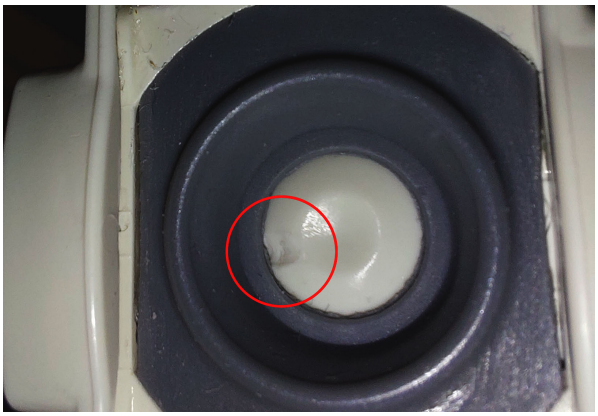

Fig. 12: Visible damage to the lower valve of trocar 24

All trocars from group 3 (trocars 7,8,9) showed an increase in leakage after manipulation for the loaded trocar inserted with a 5 mm instrument. For all three trocars combined the baseline leakage was 0.19 (0.14 – 0.23) L/min compared to 0.39 (0.31-0.42) L/min of the control measurement.

Trocar 14 from group 5 showed an increase in leakage for both unloaded and loaded measurements with a 10 mm instrument. Baseline leakage was -0.01 (-0.01–0.0) L/min and 0.0 (0.0–0.0) L/min compared to 0.15 (0.15-0.16) L/min and 0.15 (0.15-0.16) L/min for the unloaded and loaded control measurements respectively. Leakage of the empty trocar measurement also increased after manipulation from 0.0 (-0.01– 0.0) L/min to 0.15 (0.15-0.16) L/min.

All trocars from group 1 had audible leakage during the upstroke of the loaded dynamic measurement with a 10 mm instrument. Figure 13 shows a sample of both the unloaded and loaded leakage curve for manipulation with a 10 mm instrument. The showed pattern remained unchanged for the full 20 minutes of measurement data.

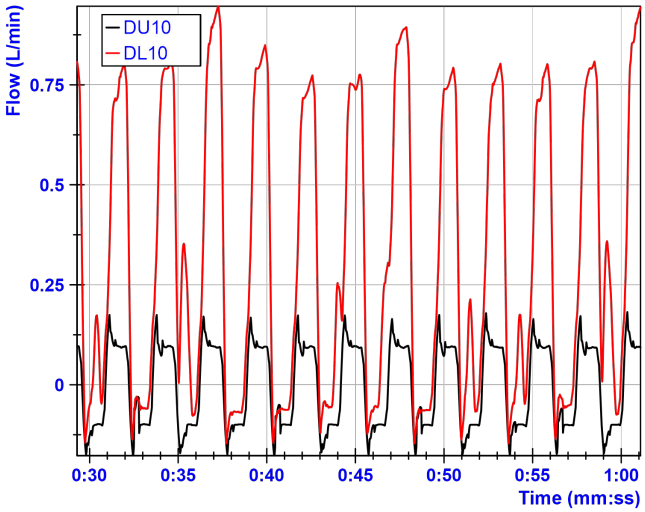

Fig. 13: Comparison of unloaded versus loaded manipulation (Trocar 1)

Figure 13 shows that leakage rates of the loaded measurement are larger during the upstroke than the unloaded measurement. For the downstroke, both curves show similar leakage rates. Therefore, additional testing was conducted by abruptly stopping the dynamic motion during the down- and upstroke and performing a one-minute static measurement. Leakage rates were 0.01 (0.00-0.01) L/min and 0.25 (0.04-0.42) L/min in the downstroke and upstroke positions respectively, for all three trocars in group 1 combined.

Trocars from group 6 showed the highest leakage rates of all trocars. A soap test showed leakage from the seal between the head and body of the trocar (Figure 14)

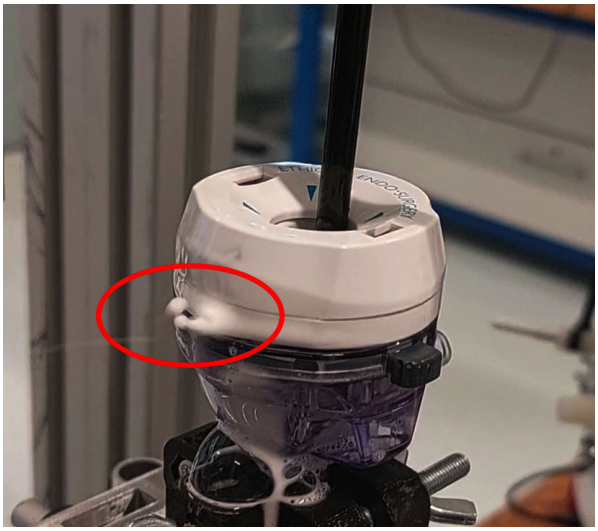

Fig. 14: Soap bubbles showing leakage between head and body of trocar 17

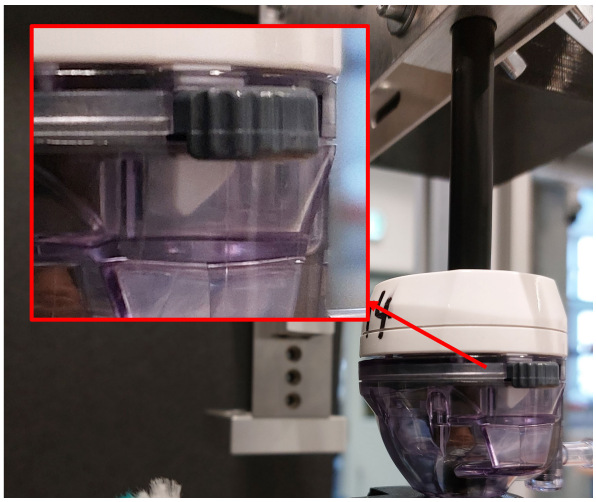

Fig. 15: View of connectors of top part trocar 17

To test the influence of connector orientation (Figure 15) on the leakage through the seal, two additional tests were performed with trocar 17. In the first test, the connectors were oriented perpendicular to the load. In the second test, the trocar was rotated 90 degrees, resulting in the connectors being oriented colinear with the trocar load. Figure 16 shows a schematic of both test conditions. A static test with a 5 mm and 10 mm instrument was conducted for one minute in both conditions.

In the colinear condition leakage rates were 0.11 (0.10-0.11) L/min and 0.13 (0.13-0.14) L/min for the 5 mm and 10 mm instruments respectively. In the perpendicular condition leakage rates were 4.39 (3.40-5.39) L/min with a 5 mm instrument and 5.42 (4.59 – 6.84) L/min with a 10 mm instrument.

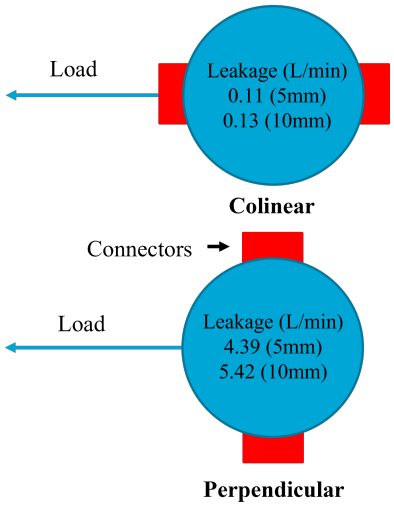

Fig. 16: Different test conditions with trocar connectors being colinear with the load (top) and perpendicular to the load (bottom)

4 Discussion

The static leakage rates after manipulation did not significantly d iffer f rom l eakage r ates b efore manipulation. Similarly, leakage during the start of manipulation did not significantly differ from leakage during the end of manipulation. Therefore, prolonged instrument manipulation did not cause an increase in gas leakage. To the author's knowledge, no other studies have researched the influence of prolonged instrument manipulation on gas leakage rates. However, Robertson et al. reported that empty trocars' leakage did not increase after short instrument manipulation and a single instrument insertion [9].

Although instrument manipulation did not increase leakage, this finding does not mean no leakage occurs through trocars. No difference will be found if leakage is already present at the baseline measurement.

Median leakage rates of empty trocars found in this study were around 0.0 – 0.01 L/min, which is in line with findings in previous research [22, 44,45]. Leakage rates of the trocars with an instrument inserted were lower than Mues et al. They reported leakage of 0.09 L/min and 0.03 L/min for a 5 mm probe and a 12 mm probe respectively [45]. Mues et al. only tested a single trocar type, which might not be representative of other trocars. Additionally, a probe instead of a laparoscopic instrument was used. A different surface roughness of the probe could have led to increased leakage.

In general, most leakage measurements were below 0.1 L/min. These leakage values could be considered minor. However, this leakage would occur continuously during surgery. A surgical procedure of two hours would still result in 12 liters of gas leakage with a leakage rate of 0.1 L/min. Besides continuous low-flow leakage, various actions in clinical practice could lead to bursts of high-flow leakage. D uring i nstrument i nsertions, leakage values up to 17 L/min and 31.3 L/min have been reported by Cahill et al. [8] and Robertson et al. [9] respectively. Also, opening the trocar stopcock results in high leakage of more than four liters per minute [8]. This is of relevance since opening the stopcock during laparoscopic surgery is considered common practice [10,46,47]. Bursts of gas leakage could potentially lead to locally high con-

centrations of harmful substances being inhaled by operating personnel. Therefore, these incidental bursts of leakage might be of large importance regarding operating personnel's safety.

Although prolonged instrument manipulation did not increase leakage, specific trocars showed increased leakage caused by different failure mechanisms. For example, one trocar developed a tear during loaded instrument manipulation. The trocar was designed such that the proximal end of the trocar included the upper valve. Therefore, forces applied to the instrument will be transmitted to the trocar valve. In other trocars, the upper valve was located more distally. Such a design limits the valve force when the instrument contacts the proximal and the distal end of the trocar. The differences in designs are illustrated in Figure 17. It is recommended to prevent upper valve placement at the proximal tip of the trocar to limit the maximum forces applied to the trocar valve.

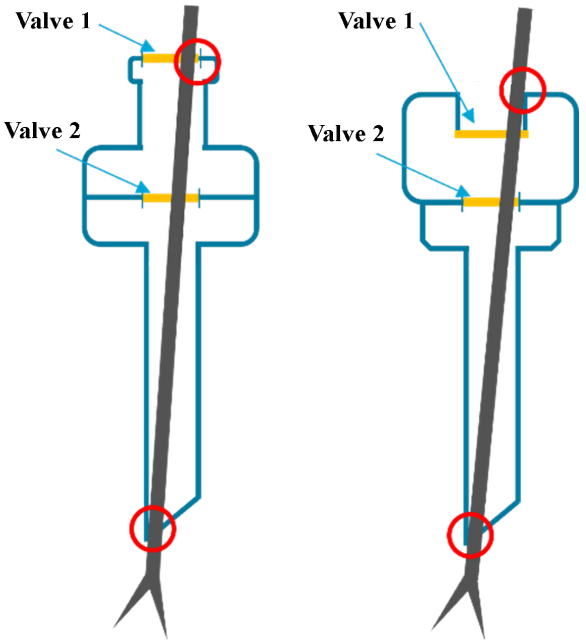

Fig. 17: Trocar with upper contact point against valve (left) and against housing (right)

Another trocar developed wear on the lower trocar valve during instrument manipulation. This trocar used a spring-loaded, hinged lower valve that automatically closes if the instrument is removed. During manipulation, the valve is pushed against the instrument shaft. Repeated axial displacement could induce wear due to increased friction from the spring-loaded mechanism. During instrument insertions, additional wear is induced when the instrument tip is pushed against the trocar valve. Loss of valve material prevents a proper seal, causing leakage of the empty trocar. With a hinged valve design, durable materials are essential. Furthermore, the spring-loaded hinge's closing force must be sufficient for a proper seal without inducing excessive friction during instrument manipulation. Other trocars with a similar mechanism of the lower valve did not show visible wear, showing a hinged valve could be a functional design. It should be noted that the instruments used during this trial had a blunt tip. If instruments with a sharp tip, such as scissors or clippers, are inserted, valve damage could occur sooner. Takano et al. presented a case where part of a trocar valve was torn off after removing laparoscopic scissors [48]. Debris of worn trocars inside the abdomen could potentially lead to a harmful situation for the patient. Therefore durability needs to be ensured in trocar designs.

Three identical 15 mm trocars were tested in this trial. They all showed increased leakage after manipulation with a 5 mm instrument. An explanation could be that the larger diameter of the trocar allows for a more angled position of the instrument inside the trocar. The inclined instrument causes an increased asymmetrical load distribution to the valve, potentially accelerating wear. Although no valve damage was visible, small alterations in the trocar valve could still lead to increased leakage. Using a 5 mm instrument in a 15 mm trocar could be needed during specific procedures requiring a larger instrument at some point in the procedure. In such a case, the largest instrument diameter determines the diameter of the trocar being used. Since only one trocar type with a 15 mm diameter was tested, additional research is needed with different trocar types to confirm this finding. Until then, it is suggested to limit the usage of a small instrument in a large trocar when possible.

One type of reusable trocar was tested three times. This trocar requires upper valve replacement after every surgery. The fact that the second measurement showed increased leakage is surprising since all replacement valves were unused. Increased leakage could not be explained by imperfections of the instrument or changing environmental cir-

cumstances since the subsequent trocar showed no increased leakage. Results from this trocar group suggest that trocars can show altering leakage rates even within a specific trocar type. Robertson et al. [9] also reported significant variations between similar trocars.

The valves of the first trocar group showed increased leakage when the instrument was stopped during the upstroke of the axial manipulation. This state causes the trocar valve to be oriented upwards (Figure 18). An explanation for increased leakage in this configuration could be that the trocar valve is pushed open by the pressure inside the container. Conversely, the valve closes when pushed against the instrument shaft if the trocar valve is oriented downwards (Figure 18). Therefore, further research and trocar development efforts should be aware that the valve orientation could influence leakage.

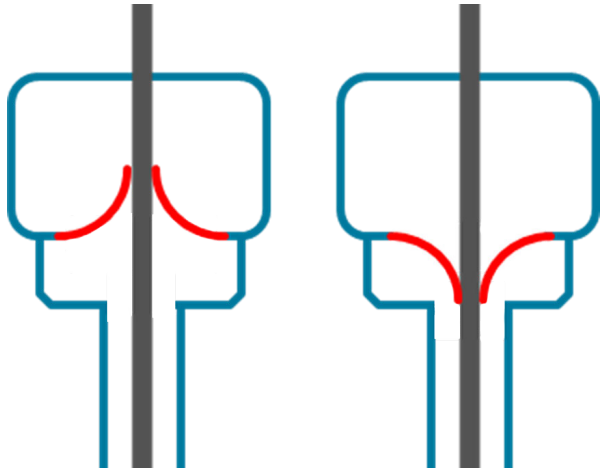

Fig. 18: Upwards valve position (left) downwards valve position (right)

Relatively high leakage rates in trocar group 6 were only present in the loaded measurements. Since leakage came from the seal between the top and bottom part, the load is suspected of pulling open the seal. This could happen due to mechanical play in the connection between the top and bottom parts. This hypothesis is confirmed by the measurements with connections perpendicular to the load. This configuration prevents pivoting of the top part, and thus the seal remains closed. Important to note is that trocars from groups 7 and 8 were of the same brand and had similar trocar designs. Nevertheless, these trocars did not show similar leakage under loading with an inserted instrument. Larger tolerances in the development or production process of trocars in group 6 could have led to increased pivoting of the top parts over the bottom, resulting in leakage. Reduced leakage after instrument manipulation in group 6 is surprising. However, leakage in these trocars was mainly caused by the opening in the seal between the top and bottom parts of the trocar. A slight change in the positioning of the top part relative to the bottom could significantly alter the leakage.

Overall multiple different leakage mechanisms exist that are trocar specific. Although commonly used trocars were included in this study, generalizing leakage mechanisms to similar trocars remains difficult.

Limitations

A total of 25 trocars were included in this study. Trocars were subdivided into groups consisting of up to three identical trocars. Group sample sizes were too small to provide a statistical comparison between different trocar groups. Furthermore, four individual trocars were tested and might not be representative of all trocars of the same type.

Using a static trocar load in combination with axial manipulation is a simplification of clinical practice. The setup results in loading a specific part of the trocar valve for a prolonged time, which could be considered a worst-case scenario. During laparoscopic surgery, load direction changes and instrument manipulation consists of a combination of pivotal, axial, and radial displacements. In this trial, leakage did not increase after manipulation despite the worst-case scenario. On the other hand, peak loads could occur in clinical practice causing damage to the trocar valve. Currently, studies presenting detailed information about the interacting force between laparoscopic instruments and trocars are lacking. Accurate force/torque measurements during surgical procedures would enable more accurate load cases in future experimental research.

In this research, only two instruments were used for manipulation. These instruments had plastic coating over the stainless steel outer tube. Instruments with a different material outer shaft could result in increased friction, causing valve

deterioration. Additionally, different instrument tips might cause more damage to trocar valves during instrument insertions.

Furthermore, only gas leakage through the trocar was tested in this study. In clinical practice, different leakage mechanisms are present simultaneously. Leakage along the trocar, through the trocar, and through instruments contribute to overall gas leakage. Consequently, this study does not provide information regarding overall gas leakage during laparoscopic surgery.

Recommendations

This research provides new insights into gas leakage during MIS. However, additional research is required to make broader claims about the safety of MIS regarding gas leakage. Three critical areas of research can be distinguished. These are particle production, particle release, and particle spread. Gas leakage through trocars is part of particle release, along with leakage between the incision and the trocar and leakage through instrument shafts. This refers to the escape of gas from the abdominal cavity. Several studies have quantified leakage through the trocar and the instrument shaft [8, 21, 22, 45, 49]. However, studies quantifying leakage between the incision and the trocars are still lacking. Therefore future research should focus on this leakage mechanism and influencing factors.

Furthermore, particle production during laparoscopy is an area of importance. Aerosol production mechanisms and their role in infection transmission must be clarified further. The importance of energy devices producing smoke particles has already been established [13, 14]. Future research should focus on reducing particle production during dissection. Limitation of particle production should be a design goal during the development of new dissection instruments.

Lastly, the third area relates to particle spread. Currently, operating room ventilation is focused on preventing surgical site infections. However, operating room ventilation could also prevent hazardous gas leakage from being inhaled by operating personnel. Modern operating theaters use air ventilation above 3000 m^3/hour [50]. Nevertheless, Hardy et al. stated that modern operating rooms could not prevent particle spread sufficiently [18]. Studies comparing different types and properties of ventilation concerning particle exposure of the operating personnel are needed. Such studies require clinical trials in certified operating theatres. Instead of preventing particle spread using airflow in the operating room, local particle removal could be promising. For example, adding a second instrument valve and applying active suction between both valves would remove leaked gas through the trocar, preventing particle spread.

Until risks related to gas leakage are clarified, operating personnel should be aware of the potential hazard and adhere to current existing guidelines to mitigate exposure as much as possible.

Conclusions

Altogether, this study shows that prolonged trocar loading did not influence gas leakage rates in dynamic and static measurements. Nevertheless, gas leakage is often present, and leakage differs significantly between trocars. Additionally, multiple failure mechanisms have been identified in this study to provide guidance during new trocar developments and as a possible starting point for future research.

References

[1] I. Alkatout, U. Mechler, L. Mettler, J. Pape, N. Maass, M. Biebl, G. Gitas, A. S. Laganà, and D. Freytag, "The development of laparoscopy—a historical overview," *Frontiers in Surgery*, vol. 8, 2021.

[2] F. Coccolini, F. Catena, M. Pisano, F. Gheza, S. Fagiuoli, S. Di Saverio, G. Leandro, G. Montori, M. Ceresoli, D. Corbella, M. Sartelli, M. Sugrue, and L. Ansaloni, "Open versus laparoscopic cholecystectomy in acute cholecystitis. systematic review and meta-analysis," *Int J Surg*, vol. 18, pp. 196–204, 2015.

[3] K. Mohiuddin and S. J. Swanson, "Maximizing the benefit of minimally invasive surgery," *J Surg Oncol*, vol. 108, no. 5, pp. 315–9, 2013.

[4] J. Reoch, S. Mottillo, A. Shimony, K. B. Filion, N. V. Christou, L. Joseph, P. Poirier,

and M. J. Eisenberg, "Safety of laparoscopic vs open bariatric surgery: a systematic review and meta-analysis," *Arch Surg*, vol. 146, no. 11, pp. 1314–22, 2011.

[5] A. Sood, C. P. Meyer, F. Abdollah, J. D. Sammon, M. Sun, S. R. Lipsitz, M. Hollis, J. S. Weissman, M. Menon, and Q. D. Trinh, "Minimally invasive surgery and its impact on 30-day postoperative complications, unplanned readmissions and mortality," *Br J Surg*, vol. 104, no. 10, pp. 1372–1381, 2017.

[6] K. S. Gurusamy, J. Vaughan, and B. R. Davidson, "Low pressure versus standard pressure pneumoperitoneum in laparoscopic cholecystectomy," *Cochrane Database Syst Rev*, no. 3, p. Cd006930, 2014.

[7] C. F. la Chapelle, W. A. Bemelman, B. M. Rademaker, T. A. van Barneveld, and F. W. Jansen, "A multidisciplinary evidence-based guideline for minimally invasive surgery.: Part 1: entry techniques and the pneumoperitoneum," *Gynecol Surg*, vol. 9, no. 3, pp. 271–282, 2012.

[8] R. A. Cahill, J. Dalli, M. Khan, M. Flood, and K. Nolan, "Solving the problems of gas leakage at laparoscopy," *Br J Surg*, vol. 107, no. 11, pp. 1401–1405, 2020.

[9] D. Robertson, F. Sterke, W. van Weteringen, A. Arezzo, Y. Mintz, F. Nickel, L. Boni, L. Baldari, T. Carus, M. Chand, H. Fuchs, F. Ficuciello, S. Marconi, G. Mylonas, Y. W. Kim, K. Nakajima, M. Schijven, P. Valdastri, C. Sagiv, P. Mascagni, P. Myśliwiec, W. Petz, F. Sánchez-Margallo, T. Horeman, and S. the Technology committee of the European Association for Endoscopic, "Characterisation of trocar associated gas leaks during laparoscopic surgery," *Surgical Endoscopy*, 2021.

[10] S. H. Choi, T. G. Kwon, S. K. Chung, and T. H. Kim, "Surgical smoke may be a biohazard to surgeons performing laparoscopic surgery," *Surg Endosc*, vol. 28, no. 8, pp. 2374–80.

[11] M. Dobrogowski, W. Wesołowski, M. Kucharska, A. Sapota, and L. S. Pomorski, "Chemical composition of surgical smoke formed in the abdominal cavity during laparoscopic cholecystectomy–assessment of the risk to the patient," *Int J Occup Med Environ Health*, vol. 27, no. 2, pp. 314–25, 2014.

[12] J. E. Fitzgerald, M. Malik, and I. Ahmed, "A single-blind controlled study of electrocautery and ultrasonic scalpel smoke plumes in laparoscopic surgery," *Surg Endosc*, vol. 26, no. 2, pp. 337–42, 2012.

[13] C. Georgesen and S. R. Lipner, "Surgical smoke: Risk assessment and mitigation strategies," *J Am Acad Dermatol*, vol. 79, no. 4, pp. 746–755, 2018.

[14] N. Mowbray, J. Ansell, N. Warren, P. Wall, and J. Torkington, "Is surgical smoke harmful to theater staff? a systematic review," *Surg Endosc*, vol. 27, no. 9, pp. 3100–7, 2013.

[15] J. Pasquier, O. Villalta, S. Sarria Lamorú, C. Balagué, R. Vilallonga, and E. M. Targarona, "Are smoke and aerosols generated during laparoscopic surgery a biohazard? a systematic evidence-based review," *Surg Innov*, vol. 28, no. 4, pp. 485–495, 2021.

[16] N. van Doremalen, T. Bushmaker, D. H. Morris, M. G. Holbrook, A. Gamble, B. N. Williamson, A. Tamin, J. L. Harcourt, N. J. Thornburg, S. I. Gerber, J. O. Lloyd-Smith, E. de Wit, and V. J. Munster, "Aerosol and surface stability of sars-cov-2 as compared with sars-cov-1," *New England Journal of Medicine*, vol. 382, no. 16, pp. 1564–1567.

[17] J. Rymarowicz, T. Stefura, P. Major, J. Szeliga, G. Wallner, M. Nowakowski, and M. Pedziwiatr, "General surgeons' attitudes towards covid-19: A national survey during the sars-cov-2 virus outbreak," *Eur Surg*, vol. 53, no. 1, pp. 5–10.

[18] N. Hardy, J. Dalli, M. F. Khan, K. Nolan, and R. A. Cahill, "Aerosols, airflow, and airspace contamination during laparoscopy," *The British journal of surgery*, vol. 108, no. 9, pp. 1022–1025.

[19] C. I. Li, J. Y. Pai, and C. H. Chen, "Characterization of smoke generated during the use of surgical knife in laparotomy surgeries," *J Air Waste Manag Assoc*, vol. 70, no. 3, pp. 324–332.

[20] H. K. Wang, F. Mo, C. G. Ma, B. Dai, G. H. Shi, Y. Zhu, H. L. Zhang, and D. W.

Ye, "Evaluation of fine particles in surgical smoke from an urologist's operating room by time and by distance," *Int Urol Nephrol*, vol. 47, no. 10, pp. 1671–8.

[21] D. Robertson, F. Sterke, W. van Weteringen, A. Arezzo, Y. Mintz, F. Nickel, and T. Horeman, "Characterisation of trocar associated gas leaks during laparoscopic surgery," *Surg Endosc*, pp. 1–10.

[22] J. M. Uecker, A. Fagerberg, N. Ahmad, A. Cohen, M. Gilkey, F. Alembeigi, and C. R. Idelson, "Stop the leak!: Mitigating potential exposure of aerosolized covid-19 during laparoscopic surgery," *Surgical endoscopy*, vol. 35, no. 1, pp. 493–501.

[23] J. Rosen, M. Solazzo, B. Hannaford, and M. Sinanan, "Task decomposition of laparoscopic surgery for objective evaluation of surgical residents' learning curve using hidden markov model," *Comput Aided Surg*, vol. 7, no. 1, pp. 49–61, 2002.

[24] J. Rosen, M. MacFarlane, C. Richards, B. Hannaford, and M. Sinanan, "Surgeon-tool force/torque signatures - evaluation of surgical skills in minimally invasive surgery," *Studies in health technology and informatics*, vol. 62, pp. 290–6, 1999.

[25] "Technical description and service instructions for electronic endoflator® model 26 4305 20, model 26 4305 20-1," Karl Storz 2011, accessed on 18-10-2022. [Online]. Available: http://www.frankshospitalworkshop.com/equipment/documents/endoscopy/service_manuals/Storz%20Endoflator%20Insufflation%20Unit%20-%20Service%20manual.pdf

[26] K. Ebina, T. Abe, M. Higuchi, J. Furumido, N. Iwahara, M. Kon, K. Hotta, S. Komizunai, Y. Kurashima, H. Kikuchi, R. Matsumoto, T. Osawa, S. Murai, T. Tsujita, K. Sase, X. Chen, A. Konno, and N. Shinohara, "Motion analysis for better understanding of psychomotor skills in laparoscopy: objective assessment-based simulation training using animal organs," *Surg Endosc*, vol. 35, no. 8, pp. 4399–4416, 2021.

[27] L. P. Aitchison, C. K. Cui, A. Arnold, E. Nesbitt-Hawes, and J. Abbott, "The ergonomics of laparoscopic surgery: a quantitative study of the time and motion of laparoscopic surgeons in live surgical environments," *Surgical Endoscopy*, vol. 30, no. 11, pp. 5068–5076.

[28] K. T. Den Boer, L. T. De Wit, J. Dankelman, and D. J. Gouma, "Peroperative time-motion analysis of diagnostic laparoscopy with laparoscopic ultrasonography," *British Journal of Surgery*, vol. 86, no. 7, pp. 951–955.

[29] M. H. Geryane, G. B. Hanna, and A. Cuschieri, "Time-motion analysis of operation theater time use during laparoscopic cholecystectomy by surgical specialist residents," *Surgical Endoscopy and Other Interventional Techniques*, vol. 18, no. 11, pp. 1597–1600.

[30] M. Gokceimam, S. Akbulut, O. Erten, B. Kahramangil, Y. S. Kim, P. P. Li, and E. Berber, "An intra-operative video comparison of laparoscopic versus robotic transabdominal lateral adrenalectomy," *International journal of medical robotics and computer assisted surgery*, vol. 17, no. 2, 2021.

[31] M. Kranzfelder, A. Schneider, A. Fiolka, D. Ing, E. Schwan, S. Gillen, D. Wilhelm, R. Schirren, S. Reiser, B. Jensen, D. Inf, and H. Feussner, "Real-time instrument detection in minimally invasive surgery using radiofrequency identification technology," *Journal of Surgical Research*, vol. 185, no. 2, pp. 704–710.

[32] H. L. Liu, T. Kinoshita, A. Tonouchi, A. Kaito, and M. Tokunaga, "What are the reasons for a longer operation time in robotic gastrectomy than in laparoscopic gastrectomy for stomach cancer?" *Surgical endoscopy and other interventional techniques*, vol. 33, no. 1, pp. 192–198, 2019.

[33] D. J. Miller, C. A. Nelson, and D. Oleynikov, "Shortened or time and decreased patient risk through use of a modular surgical instrument with artificial intelligence," *Surgical Endoscopy*, vol. 23, no. 5, pp. 1099–1105.

[34] L. Stotz, R. Joukhadar, A. Hamza, F. Thangarajah, D. Bardens, I. Juhasz-Böss, E. F. Solomayer, M. P. Radosa, and J. C. Radosa, "Instrument usage in laparo-

scopic gynecologic surgery: a prospective clinical trial," *Archives of Gynecology and Obstetrics*, vol. 298, no. 4, pp. 773–779.

[35] E. Sutton, Y. Youssef, N. Meenaghan, C. Godinez, Y. Xiao, T. Lee, D. Dexter, and A. Park, "Gaze disruptions experienced by the laparoscopic operating surgeon," *Surgical Endoscopy*, vol. 24, no. 6, pp. 1240–1244.

[36] M. V. U. Torney, S. Aghlmandi, J. Zeindler, D. Nowakowski, C. A. Nebiker, C. Kettelhack, R. Rosenthal, R. A. Droeser, S. D. Soysal, H. Hoffmann, and R. Mechera, "High-resolution standardization reduces delay due to workflow disruptions in laparoscopic cholecystectomy," *Surgical endoscopy and other interventional techniques*, vol. 32, no. 12, pp. 4763–4771, 2018.

[37] M. V. U. Torney, S. Dell-Kuster, H. Hoffmann, U. von Holzen, D. Oertli, and R. Rosenthal, "Microcomplications in laparoscopic cholecystectomy: impact on duration of surgery and costs," *Surgical endoscopy and other interventional techniques*, vol. 30, no. 6, pp. 2512–2522, 2016.

[38] "Haf series honeywell zephyr™ digital airflow sensors," Honeywell International Inc. 2021, accessed on 18-10-2022. [Online]. Available: https://prod-edam.honeywell.com/content/dam/honeywell-edam/sps/siot/en-gb/products/sensors/airflow-sensors/amplified/honeywell-zephyr-haf-series-low-flow/\documents/sps-siot-zephyr-digital-airflow-10-slpm\-300-slpm-datasheet-008268-5-en-ciid-144883.pdf

[39] "Data sheet rudolph volume calibration syringes," Hans Rudolph inc. 2020, accessed on 18-10-2022. [Online]. Available: https://drive.google.com/file/d/1P49PswNpeMOihw8X8TbFJzcjjRl93kmn/view

[40] "Abp series basic board mount pressure sensors," Honeywell International Inc. 2020, accessed on 18-10-2022. [Online]. Available: https://eu.mouser.com/datasheet/2/187/honeywell_sensing_basic_board_mount_pressure_abp_s-1662208.pdf

[41] "Ultrasonic ranging module hc - sr04," SparkFun Electronics 2022, accessed on 18-10-2022. [Online]. Available: https://cdn.sparkfun.com/datasheets/Sensors/Proximity/HCSR04.pdf

[42] "Arduino uno r3 datasheet," 2022, accessed on 18-10-2022. [Online]. Available: https://docs.arduino.cc/static/efc945f45b17ec9975d54c9ba601b4a9/A000066-datasheet.pdf

[43] "Datasheet stc31 co2 sensor based on thermal conductivity," Sensirion Inc. 2020, accessed on 18-10-2022. [Online]. Available: https://sensirion.com/media/documents/7B1D0EA7/61652CD0/Sensirion_Thermal_Conductivity_Datasheet_STC31_D1_1.pdf

[44] C. D. R. J. W. C. Cepress J.M., John F Cummings and G. A. Tommaselli, "Comparison of trocar performance in consideration of the covid-19 pandemic." *Medical Devices and Diagnostic Engineering*, 2020.

[45] A. C. Mues, G. Haramis, C. Casazza, Z. Okhunov, K. K. Badani, and J. Landman, "Prospective randomized single-blinded in vitro and ex vivo evaluation of new and reprocessed laparoscopic trocars," *J Am Coll Surg*, vol. 211, no. 6, pp. 738–43, 2010.

[46] D. Vaishnav and B. Patel, "Laparoscopic gastrointestinal surgery during covid-19 pandemic: Single-center experience," *J Laparoendosc Adv Surg Tech A*, vol. 31, no. 4, pp. 455–457, 2021.

[47] Y. Vigneswaran, V. N. Prachand, M. C. Posner, J. B. Matthews, and M. Hussain, "What is the appropriate use of laparoscopy over open procedures in the current covid-19 climate?" *J Gastrointest Surg*, vol. 24, no. 7, pp. 1686–1691, 2020.

[48] K. Takano, W. Takao, K. Abe, and K. Urushigawa, "Experience of valve breakage of the trocar used for laparoscopic surgery," *Japanese journal of gynecologic and obstetric endoscopy*, vol. 35, no. 1, pp. 153–157, 2019.

[49] M. S. Baggish, "Comparison of smoke and sprayback leakage from two different trocar sleeves during operative laparoscopy," *Journal of Gynecologic Surgery*, vol. 9, no. 2, pp.

65–76.

[50] J. L. A. Lans, N. M. C. Mathijssen, A. Bode, J. J. van den Dobbelsteen, M. van der Elst, and P. G. Luscuere, "Operating room ventilation systems: recovery degree, cleanliness recovery rate and air change effectiveness in an ultra-clean area," *J Hosp Infect*, vol. 122, pp. 115–125, 2022.

[51] N. Bevan, J. Carter, J. Earthy, T. Geis, and S. Harker, *What are user requirements? Developing an ISO standard*, 2018.

[52] J. Rosen, J. D. Brown, L. Chang, M. Barreca, M. Sinanan, and B. Hannaford, "The bluedragon - a system for measuring the kinematics and dynamics of minimally invasive surgical tools in-vivo," in *Proceedings 2002 IEEE International Conference on Robotics and Automation (Cat. No.02CH37292)*, vol. 2, Conference Proceedings, pp. 1876–1881 vol.2.

Appendix A: Requirements experimental setup

An experimental setup is needed to investigate the research goal. Starting from the research goal a set of user requirements has been developed. The user requirements state what the experimental setup should be capable of from the researcher's perspective. They define the capability and usability of the experimental setup [51]. The user requirements (Table A1) outline what the experimental setup has to achieve. They bridge the gap between the general research goal and specific system requirements. The system requirements (Table A2) are developed to fulfill the user requirements. System requirements are specific and measurable and can thus be used during the design and evaluation of the setup. Information acquired from medical specialists, engineers, literature research, and pilot testing form the basis of both user and system requirements.

Table A1: User requirements

Level	Identifier	Description
General		
1.1	UR.Safety	The system shall be safe for the user
1.2	UR.Size	The system shall have a limited footprint to fit on a lab table
1.3	UR.Reuse	The system shall be reusable for multiple experiments
Modeled abdomen		
1.4	UR.Abdomen	The system shall include a model of a sealed abdominal cavity
1.5	UR.Access	The modeled abdominal cavity shall be accessible without damaging the system
1.6	UR.Pressure	The system shall be filled with CO_2 and be able to keep a preset constant pressure in the abdominal cavity similar to a pneumoperitoneum
1.7	UR.Trocar	The system shall allow for placement of a trocar with various sizes in the abdominal cavity
1.8	UR.Visual	The user shall be able to monitor the inside of the modeled abdomen during measurements
Measurements		
1.9	UR.FlowSens	The system shall be able to measure the flow of escaped gas from the modeled intra-abdominal cavity through the trocar
1.10	UR.PressureSens	The system shall be able to measure the pressure inside the modeled abdomen
1.11	UR.DistanceSens	The system shall be able to track the displacement of the manipulated instrument
1.12	UR.UI	The system shall display real-time measurement values
1.13	UR.Store	The system shall be able to store measurement data on demand
1.14	UR.Time	The system shall be able to measure over a longer duration
Instrument handling		
1.15	UR.Instrument	The system shall be able to hold various instruments
1.16	UR.Alignment	The system shall allow for aligning the instrument with the trocar
1.17	UR.Manipulation	The interacting load between trocar and instrument shall be similar to clinical practice
1.18	UR.ControlAxial	The axial motion of the laparoscopic instrument shall be controllable
1.19	UR.ControlLoad	The interacting force/moment between the trocar and instrument shall be controllable at a constant value
1.20	UR.Exchange	The system shall allow for repeated removal and insertion of a laparoscopic instrument

Table A2: System requirements

Level	Identifier	Description	Variable	Value	Unit	Parent	Source	Method of verification	Status	Comment
General										
2.1	SR.Safety	The system shall have an emergency switch to stop all moving parts				UR.Safety		Y/N (Yes or No)	Verified	Festo controller emergency stop
2.2	SR.Size	The dimensions of the system shall not exceed X by Y and a height of Z	X	45	cm	UR.Size	Based on Thorlabs plate under linear stage	Measurement dimensions	Verified	Final dimensions X: 38.5 cm; Y: 42cm; Z: 26cm
			Y	45	cm					
			Z	30	cm					
2.3	SR.Reuse	The system shall be able to be reused X times without replacing components	X	30		UR.Reuse	Trocar nozzle torn after 4 trocars	Test run with changing (same) trocar 30 times in set up. Visual check for damage	**Failed**	Spare silicon nozzle needed, can be replaced within 5 minutes
2.4	SR.Time	The system shall be able to run loaded uninterrupted for X	X	40	minutes	UR.Time	Protocol max. 20 minutes of continuous loaded testing	Test run of at least 40 minutes. Visual check for damage	Verified	
Modelled abdomen										
2.5	SR.Airtight	The abdominal cavity shall hold a constant pressure of X for Y minutes using no more than Z liters of CO2	X	2000	Pa	UR.Abdomen	2000 pa = 15 mmHg used for experiment	Soap bubble test. 30 minutes sealed testing, read flow from insufflator	Verified	No bubbles detectable, after 30 minutes < 0.1 L leakage
			Y	30	Minutes					
			Z	3	Liter		Equal to model of pilot testing			
2.6	SR.Assembly	The model shall be accessible within X without damaging components	X	5	Minutes	UR.Access	Needed to adjust wiring/remove sensors.	Time disassembly time	Verified	
2.7	SR.Pressure	The model shall be able to maintain a constant pressure in the range of X set with increments of Y	X	1067-2266	Pa	UR.Pressure	Equal to 8-17 mmHg in range of protocol	Intra-abdominal pressure measurement	Verified	Karl Storz 264305 20 can be set in a range of 0 - 30 mmHg with 1 mmHg increments
			Y	133	Pa		Equal to 1 mmHg, similar to most commercially available insufflator			
2.8	SR.Volume	The model shall have a volume of X	X	10	Liter	UR.Abdomen	Volume abdomen human 3.5-5 liter additional volume to accommodate electronics without need for high volumes of CO2 to saturate.[1]	Calculate based on dimensions	Verified	Final volume 10 liters
2.9	SR.Flow Sensor	The model shall be able to house a flow sensor				UR.FlowSens		Y/N	Verified	
2.10	SR.Arduino	The model shall be able to house a microcontroller				UR.PressureSens, UR.FlowSens		Y/N	Verified	

2.11	SR.Pressure Sensor	The model shall be able to house a differential pressure sensor				UR.Pressure Sens		Y/N	Verified	
2.12	SR.Trans-parent	The modeled abdomen shall be made of see through material				UR.Visual	To be able to see inside the model during testing	Y/N	Verified	
2.13	SR.Fixation	The modeled abdomen shall be able to be fixed to a Thorlabs plate with M6 bolts spaced X apart	X	25	mm	UR.Size	Currently present under linear stage	Y/N	Verified	
2.14	SR.Through Hole	The model shall have X additional through holes	X	3		UR.Pressure, UR.PressureSens, UR.FlowSens	1: gas supply; 2:usb Arduino; 3: pressure sensor	Y/N	Verified	
2.15	SR.Access	The model shall have a sealable access opening of X by Y	X	100	mm	UR.Access	Based on dimensions Arduino and flow sensor and grant access by hand	Y/N	Verified	Two access port (130x100 and 80x60)
			Y	60	mm					
2.16	SR.Port	The abdominal cavity shall have an access port to allow trocar placement with diameters of X to Y	X	10	mm	UR.Trocar	These sizes are currently available for testing	Y/N	Verified	
			Y	15	mm					
2.17	SR.PortROM	The port in the abdominal model shall allow for a pivotal range of motion of the trocar from X to Y	X	0	Degrees	UR.Trocar	Trocar is slightly angled during loading	Measure using ImageJ *(Version 1.53[e] – Wayne Rasband and contributors, National Institutes of Health)*	Verified	Final angle 22 degrees
			Y	5	Degrees					
2.18	SR.Alignment	The modeled abdomen shall be able to align the trocar with the instrument in a plane of X by Y with an accuracy of Z	X	10	mm	UR.Alignment	Allow for precise centering of the instrument inside the trocar	Measure using ruler	Verified	Front/back in instrument holder, left/right shift linear stage
			Y	10	mm					
			Z	3	mm					
Gas supply										
2.19	SR.Gas	The abdominal cavity shall be saturated with CO2 with stable concentration within X	X	1	%	UR.Pressure	Concentration should be as constant as possible to have accurate flow measurements	Flush abdominal model, test [CO2] with 100% CO2 sensor	Verified	
2.20	SR.Inflation Flow	The abdominal cavity shall be inflated with a flow of X in case of pressure drop	X	15	L/min	UR.Pressure		Check settings/test with flow sensor	Verified	Common setting in clinical practice (Interviews) Should compensate most leakage from pilot study
2.21	SR.Insufflator	The insufflator device shall be certified to be used for laparoscopic surgery				UR.Safety, UR.Pressure		Y/N	Verified	Ensure similar pressure control to clinical practice
Instrument control										

2.22	SR.Axial	The instrument shall be able to move X in the axial direction measured from the abdominal port		±60	mm	UR.Manipulation, UR.ControlAxial		Measure using ruler/linear stage values	Verified	
2.23	SR.Axial Control Displacement	The displacement of the instrument shall be able to be controlled with an accuracy of X	X	1	mm	UR.Manipulation, UR.ControlAxial		Datasheet linear stage	Verified	
2.24	SR.Axial Control Velocity	The velocity of the instrument shall be able to be controlled in a range from X to Y	X	0	mm/s	UR.Manipulation, UR.ControlAxial		Datasheet linear stage	Verified	
			Y	50	mm/s		[2]	Camera and ruler or read linear stage values		Average in literature around 20 mm/s
2.25	SR.Instrument Diam	The system shall be able to hold both instruments with diameters of X and Y	X	5		UR.Instrument		Measure minimal and maximal diameter, Y/N	Verified	Two separate instruments holders present
			Y	10						
2.26	SR.Instrument Length	The system shall be able to hold instruments with a shaft length up to X	X	370	mm	UR.Instrument	Used instruments are 370mm	Measure maximal length, Y/N	Verified	
2.27	SR.Exchanges Stroke	The tip of the instrument shall be able to be retracted X above the trocar opening		5	mm	UR.Exchange	This guarantees full removal of the instrument tip	Measure using ruler/linear stage values	Verified	
2.28	SR.Exchanges Frequency	The system shall be able to insert and retract an instrument at least X times		40		UR.Exchange	Exchanges differ per procedure, 40/hour is top of reported values. [3-5]	Pilot study, visual inspection	Verified	
Trocar										
2.29	SR.Moment	The trocar shall be able to be loaded with a constant moment perpendicular to the trocar ranging from X to Y	X	0	Nm	UR.ControlLoad	[6-10]	Force gauge	Verified	
			Y	2	Nm			Force gauge		
2.30	SR.RadialForce Accuracy	The applied moment shall be controllable with an accuracy of X	X	0.1	Nm	UR.ControlLoad		Scale	Verified	Force applied with weight, continuous adjustment with metal chips
2.31	SR.LoadSpacing	The load shall be applied at X of the fixed point of rotation repeatably	X	5	cm	UR.ControlLoad			Verified	Custom spacers allowed precise spacing
Measurement										
2.32	SR.Flow Range	The leakage flow shall be measurable within a range of X	X	0-40	L/min	UR.FlowSens	[6, 11-14]	Dataheet sensor	Verified	Comparable to max in literature
2.33	SR.Flow Resolution	The flow measurement resolution shall be within X	X	0.05	L/min	UR.FlowSens		Dataheet sensor	Verified	
2.34	SR.Flow Accuracy	The flow measurement accuracy shall be within X	X	0.1	L/min	UR.FlowSens		Dataheet sensor	Verified	
2.35	SR.Pressure Sensor	The pressure shall be measurable over a range of X	X	0-25	mmHg	UR.PressureSens	[15]	Dataheet sensor	Verified	
2.36	SR.Pressure Resolution	The pressure measurement resolution shall be within X	X	0.1	mmHg	UR.PressureSens		Dataheet sensor	Verified	

2.37	SR.Pressure Accuracy	The pressure measurement accuracy shall be within X	X	0.2	mmHg	UR.PressureSens				
2.38	SR. Measurement Frequency	Measurements shall be taken with a frequency of X	X	40	Hz	UR.UI		Y/N	Verified	
2.39	SR. Measurement Display	Measurement values shall be displayed and plotted real-time				UR.UI		Y/N	Verified	
2.40	SR. Measurement Storage	Measurement values shall be able to be stored locally on a storage device				UR.Store	Needed for data analysis	Y/N	Verified	
2.41	SR.Distance Range	The axial displacement of the instrument shall be tracked within X	X	0-50	cm	UR.DistanceSens		Ruler	Verified	
2.42	SR.Distance Resolution	The axial displacement shall be measured with a resolution of X	X	1	cm	UR.DistanceSens		Analyse sensor data	Verified	
2.43	SR.CO2Range	The concentration CO2 shall be measured in a range of X	X	0-100	% Volume	UR.Pressure		Datasheet	Verified	
2.44	SR.CO2 Resolution	The concentration CO2 shall be measured with a resolution of X	X	0.5	%	UR.Pressure		Datasheet	Verified	

[1] G. Phillips, R. Garry, C. Kumar, and H. Reich, "How much gas is required for initial insufflation at laparoscopy?," *Gynaecological Endoscopy,* vol. 8, pp. 369-374, 12/25 2001, doi: 10.1046/j.1365-2508.1999.00342.x.

[2] K. Ebina *et al.*, "Motion analysis for better understanding of psychomotor skills in laparoscopy: objective assessment-based simulation training using animal organs," (in eng), *Surg Endosc,* vol. 35, no. 8, pp. 4399-4416, Aug 2021, doi: 10.1007/s00464-020-07940-7.

[3] L. P. Aitchison, C. K. Cui, A. Arnold, E. Nesbitt-Hawes, and J. Abbott, "The ergonomics of laparoscopic surgery: a quantitative study of the time and motion of laparoscopic surgeons in live surgical environments," (in eng), *Surg Endosc,* vol. 30, no. 11, pp. 5068-5076, Nov 2016, doi: 10.1007/s00464-016-4855-4.

[4] L. Stotz *et al.*, "Instrument usage in laparoscopic gynecologic surgery: a prospective clinical trial," (in eng), *Arch Gynecol Obstet,* vol. 298, no. 4, pp. 773-779, Oct 2018, doi: 10.1007/s00404-018-4867-5.

[5] D. J. Miller, C. A. Nelson, and D. Oleynikov, "Shortened OR time and decreased patient risk through use of a modular surgical instrument with artificial intelligence," (in eng), *Surg Endosc,* vol. 23, no. 5, pp. 1099-105, May 2009, doi: 10.1007/s00464-008-0321-2.

[6] J. F. C. Cepress J.M., Crystal D Ricketts, Jeffrey W Clymer* and Giovanni A Tommaselli, " Comparison of trocar performance in consideration of the COVID-19 pandemic. ," *Medical Devices and Diagnostic Engineering,* 2020, doi: 10.15761/MDDE.1000129.

[7] T. Horeman, J. Dankelman, F. W. Jansen, and J. J. van den Dobbelsteen, "Assessment of laparoscopic skills based on force and motion parameters," (in eng), *IEEE Trans Biomed Eng,* vol. 61, no. 3, pp. 805-13, Mar 2014, doi: 10.1109/tbme.2013.2290052.

[8] J. Rosen, J. D. Brown, L. Chang, M. Barreca, M. Sinanan, and B. Hannaford, "The BlueDRAGON - a system for measuring the kinematics and dynamics of minimally invasive surgical tools in-vivo," in *Proceedings 2002 IEEE International Conference on Robotics and Automation (Cat. No.02CH37292)*, 11-15 May 2002 2002, vol. 2, pp. 1876-1881 vol.2, doi: 10.1109/ROBOT.2002.1014814.

[9] J. Rosen, M. MacFarlane, C. Richards, B. Hannaford, and M. Sinanan, "Surgeon-tool force/torque signatures - Evaluation of surgical skills in minimally invasive surgery," *Studies in health technology and informatics,* vol. 62, pp. 290-6, 02/01 1999, doi: 10.3233/978-1-60750-906-6-290.

[10] J. Rosen, M. Solazzo, B. Hannaford, and M. Sinanan, "Task decomposition of laparoscopic surgery for objective evaluation of surgical residents' learning curve using hidden Markov model," (in eng), *Comput Aided Surg,* vol. 7, no. 1, pp. 49-61, 2002, doi: 10.1002/igs.10026.

[11] R. A. Cahill, J. Dalli, M. Khan, M. Flood, and K. Nolan, "Solving the problems of gas leakage at laparoscopy," (in eng), *Br J Surg,* vol. 107, no. 11, pp. 1401-1405, Oct 2020, doi: 10.1002/bjs.11977.

[12] A. C. Mues, G. Haramis, C. Casazza, Z. Okhunov, K. K. Badani, and J. Landman, "Prospective randomized single-blinded in vitro and ex vivo evaluation of new and reprocessed laparoscopic trocars," (in eng), *J Am Coll Surg,* vol. 211, no. 6, pp. 738-43, Dec 2010, doi: 10.1016/j.jamcollsurg.2010.08.003.

[13] D. Robertson *et al.*, "Characterisation of trocar associated gas leaks during laparoscopic surgery," *Surgical Endoscopy,* 2021/11/03 2021, doi: 10.1007/s00464-021-08807-1.

[14] J. M. Uecker *et al.*, "Stop the leak!: Mitigating potential exposure of aerosolized COVID-19 during laparoscopic surgery," (in eng), *Surgical endoscopy,* vol. 35, no. 1, pp. 493-501, 2021, doi: 10.1007/s00464-020-08006-4.

[15] J. Radosa *et al.*, "Impact of different intraoperative CO2 pressure levels (8 and 15 mmHg) during laparoscopic hysterectomy performed due to benign uterine pathologies on postoperative pain and arterial pCO2: a prospective randomised controlled clinical trial," *BJOG: An International Journal of Obstetrics & Gynaecology,* vol. 126, no. 10, pp. 1276-1285, 2019, doi: https://doi.org/10.1111/1471-0528.15826.

Appendix B: Development experimental setup

An experimental setup has been developed using the system requirements (Appendix A).

Acrylic container

To mount the trocar, a custom container was designed with a height of 250 mm and a width of 200 x 200 mm to fit to the baseplate of the linear stage. The container was assembled from clear laser-cut acrylic plates to allow monitoring of the instrument tip and electronics during the experiment. A stepped profile was added to the edges of the acrylic plates to ensure alignment, ease assembly, and improve structural integrity. A wall thickness of 5mm was chosen to obtain low compliance, preventing deformation of the model when pressurized and during instrument manipulation. Container deformation was an issue during pilot testing. Holes were added to the baseplate to align and fix the container to the threaded baseplate of the linear stage. Acrylic parts were glued together using Acrifix® 1R 0192 (Röhm GmbH, Weiterstadt, Germany). An overview of the acrylic container including access lids, through holes, and trocar mount is shown in Figure B1.

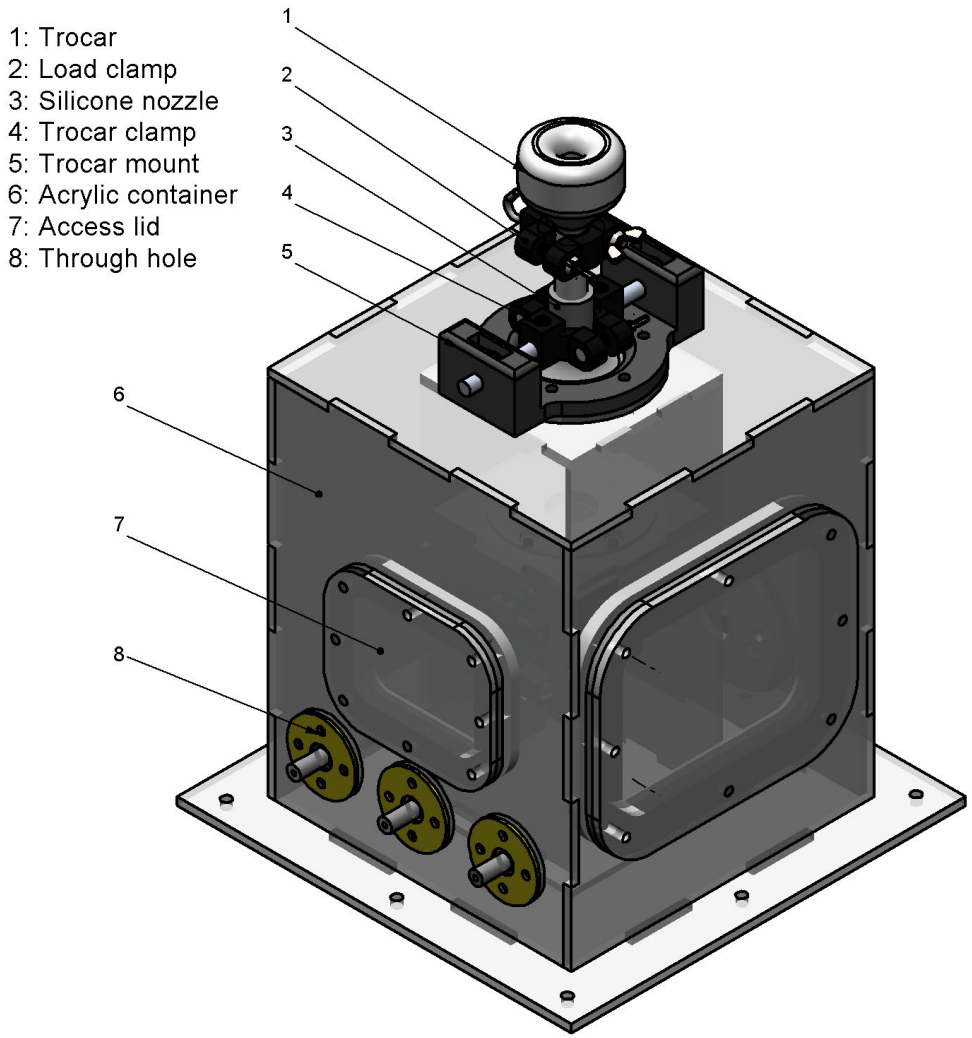

Fig. B1: Overview acrylic container with trocar mount

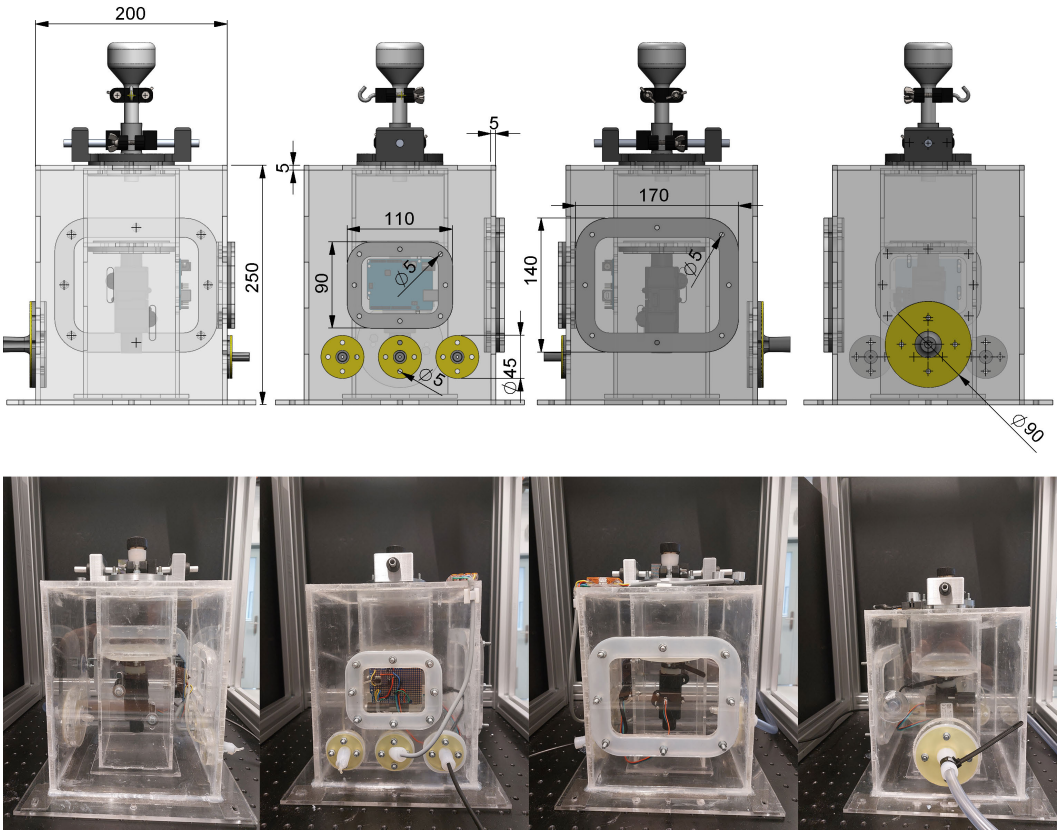

Fig. B2: Side views of the acrylic container with dimensions. Final realization (below)

An overview with some critical dimensions and the final realization of the container is shown in Figure B2.

Through holes

Multiple through holes were added to accommodate the trocar, wiring, and insufflation tube. An example of a through-hole assembly is shown in Figure B3.

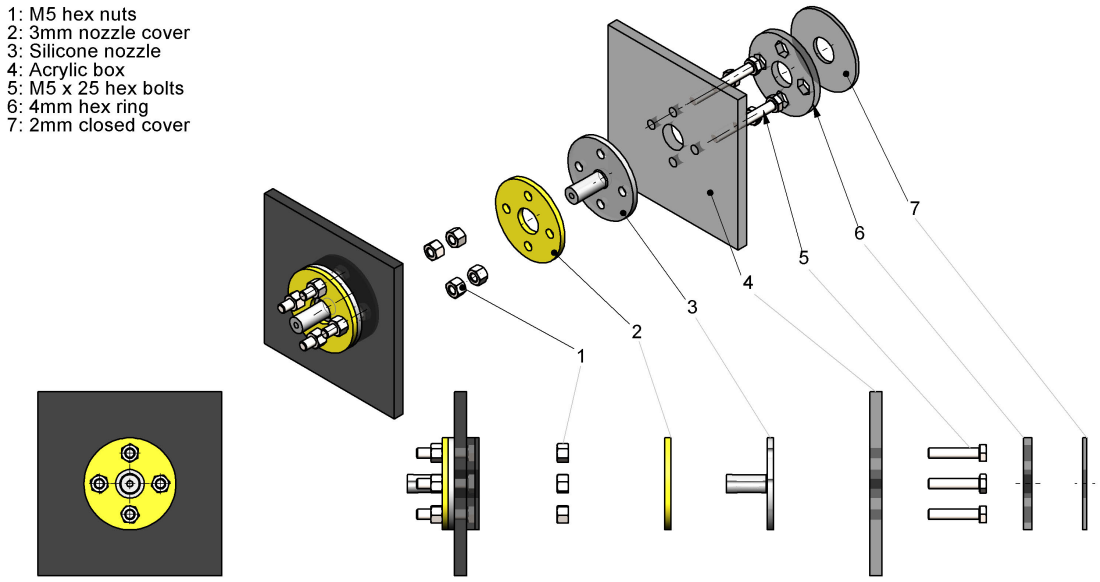

Fig. B3: Through hole assembly

The hex bolts (5) were embedded in an acrylic ring (6) to lock their rotation. A cover ring (7) was glued to the back to prevent gas leakage through the bolt holes. The hex ring was glued to the inside of the acrylic container. Nozzles were designed in SolidWorks. The nozzle was used to develop a mold. The mold was 3D printed, and two-component EcoflexTM Smooth-on P silicone with Shore 00-50 was used to pour the nozzle. The poured mold was degassed in a vacuum chamber. The access lids were sealed airtight using a similar design as the through hole assembly from figure B3.

Sensor Mount

The sensor mount is shown in Figure B4 The flow sensor was secured and placed in line with the trocar tip. This allowed for trocar tip motion without distorting flow measurements. Additionally, the inner structure improved the stiffness of the container and served as a mount for the Arduino UNO R3 microcontroller.

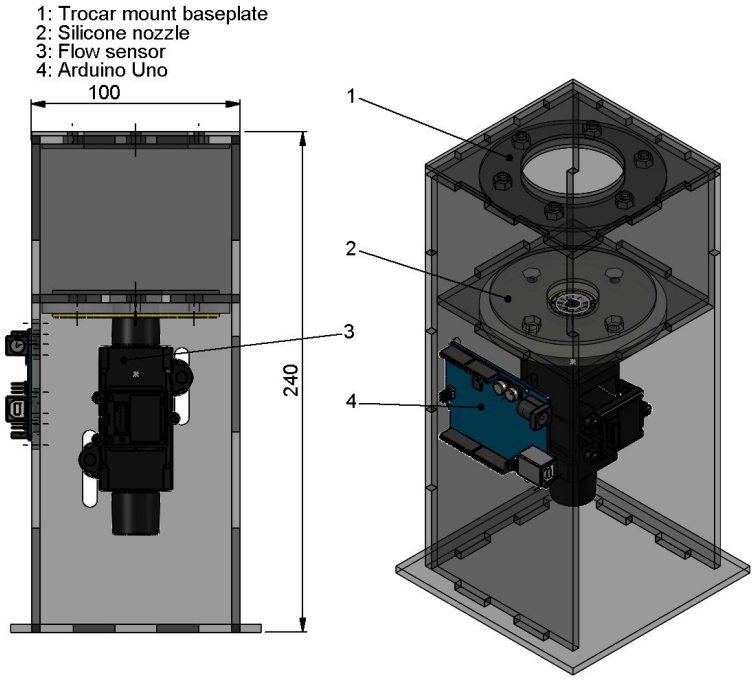

Fig. B4: Sensor mount with flow sensor and microcontroller

Flow sensor

A Honeywell Zephyr, HAFUHH0050L4AXT (Honeywell International Inc., Charlotte, North Carolina, USA) flow sensor was used to measure the leakage flow (Figure B5). Specifications of the flow sensor are available in the datasheet [39]

Fig. B5: Flow sensor

Pressure sensor

A Honeywell ABPMRRN060MGAA5 (Honeywell International Inc., Charlotte, North Carolina, USA) pressure sensor was used to measure the differential pressure between the environment and the inside of the acrylic container (Figure B6). Specifications of the pressure sensor are available in the datasheet [40]

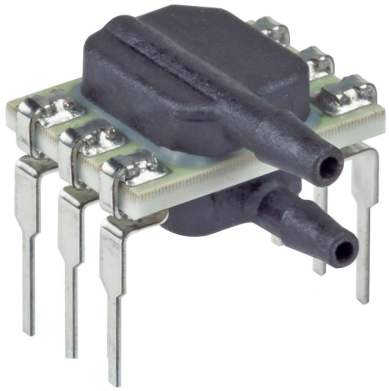

Fig. B6: Pressure sensor

Distance sensor

A HC-SR04 (SparkFun Electronics, Niwot, Colorado, USA) distance sensor was used to measure the distance between the acrylic container and the linear stage instrument mount (Figure B7). Only relative distances were of interest to monitor the displacement of the instrument. Leakage rates could therefore be correlated with the downstroke and upstroke. Specifications of the distance sensor are available in the datasheet [41]

Fig. B7: Distance sensor

Trocar mount

A trocar mount was added to the acrylic box to accommodate the trocar. The mount is shown in Figure B8.

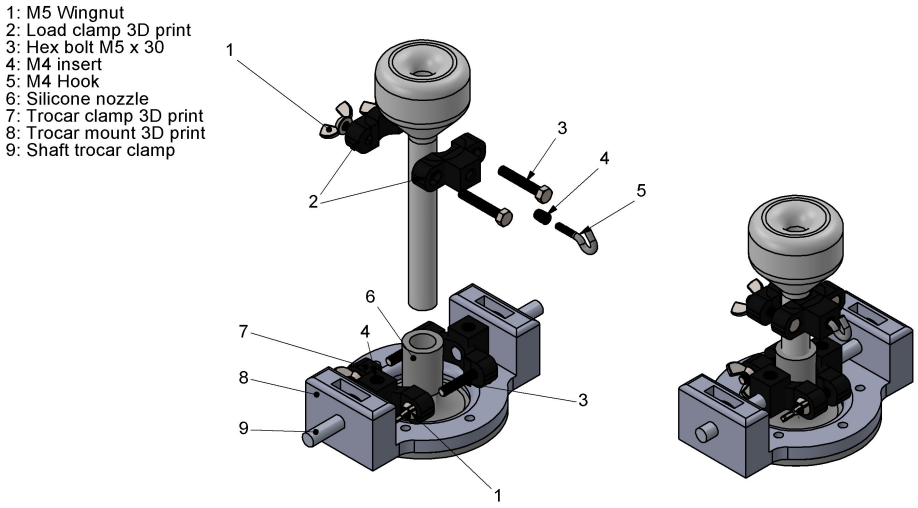

Fig. B8: Trocar mount assembly

The trocar was mounted in a silicone nozzle (6) to prevent leakage between the trocar and the trocar mount. The pivot point of the trocar was fixed with two clamps (4) to allow for a constant load on all tested trocars. Pivoting was enabled by connecting both trocar clamps to a shaft (9) that would rotate freely. A 3D printed mount (8) was developed to hold the shafts and allow for centering the trocars in the trocar nozzle. The trocar was fixated by tightening the wingnuts (1). A second clamp was designed to apply a load to the trocar (2). The clamp was attached to the trocar using M5 bolt and wingnuts. To ensure a spacing of 50mm between the pivot point and the origin of the applied load a custom spacer was developed using part measurements in SolidWorks. This setup allowed for a rigid fixture of trocars with varying diameters while maintaining convenient trocar exchange. All clamps were 3D printed with 100% density to ensure structural integrity. The realization of the design is shown in Figure B9.

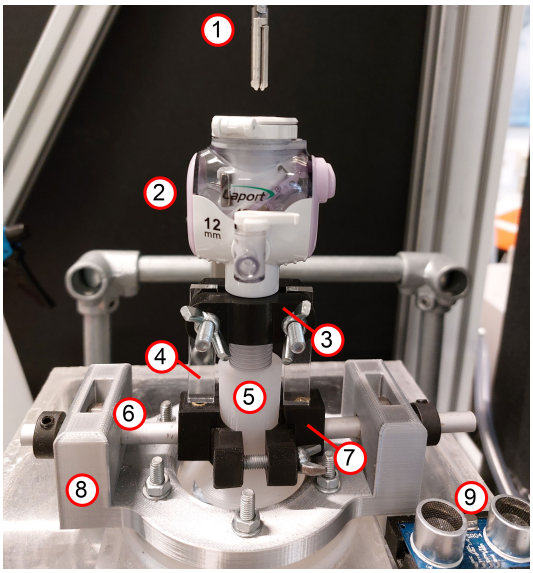

Fig. B9: Trocar mount subassembly. 1: Instrument tip, 2: Trocar, 3: Load clamp, 4: Spacer, 5:Silicone nozzle, 6: Shaft trocar clamp, 7: Trocar clamp, 8: Trocar mount, 9: Distance sensor

Load application

The setup to apply the load to the trocar is shown in Figure B10. The load was applied using a stiff rope with a weight attached at the end. A custom weight was developed composted of a baseplate with a 3D printed container (4). The container could be filled with metal chips for continuous adjustment of the applied load. A pulley (2) was attached to a rigid metal frame (3) to apply a horizontal load using a weight. The metal frame was fixed to the linear stage baseplate. To ensure a 90-degree angle, a custom spacer was used to position the pulley (Figure B10, right).

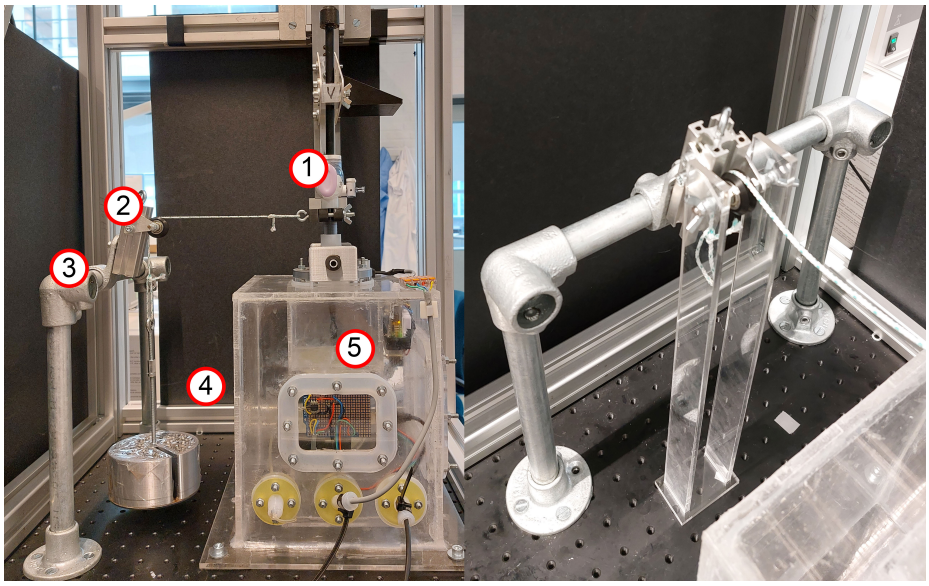

Fig. B10: Load application. 1: Trocar, 2: Pulley with rope 3: Metal support frame 4: Weight, 5:Acrylic container

Instrument mount linear stage

A custom mount for the linear stage was designed to mount the laparoscopic instrument (Figure B11). Two laser-cut aluminum plates spaced at 20 mm with square tubing were used. The handle of the instrument was removed and the end of the shaft was capped to prevent leakage through the instrument. A connector was developed to attach the instrument to the mount (Figure B11, right). The instrument was clamped in the connector with set screws to enable adaptation of the instrument length. The slotted opening in the aluminum plates allowed for the alignment of the instrument to the center of the trocar. A 3D printed flat surface was attached to the mount to provide a reference for the distance sensor.

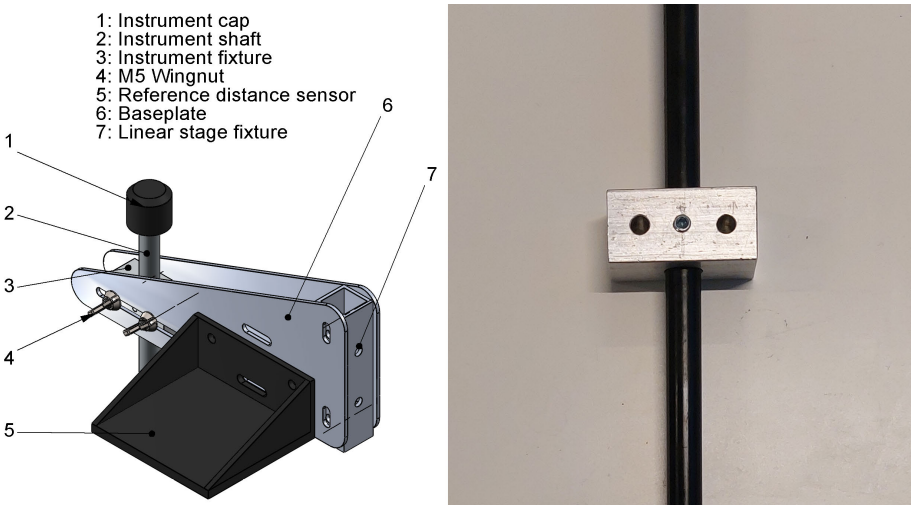

Fig. B11: Instrument mount with reference for distance sensor (left) instrument mounting connector (right)

Appendix C: Calculation trocar load

The trocar load applied during testing should be representative of clinical practice. Rosen et al. measured forces/torques at the instrument handle (Figure C1) during cholecystectomy in pigs [23, 24, 52].

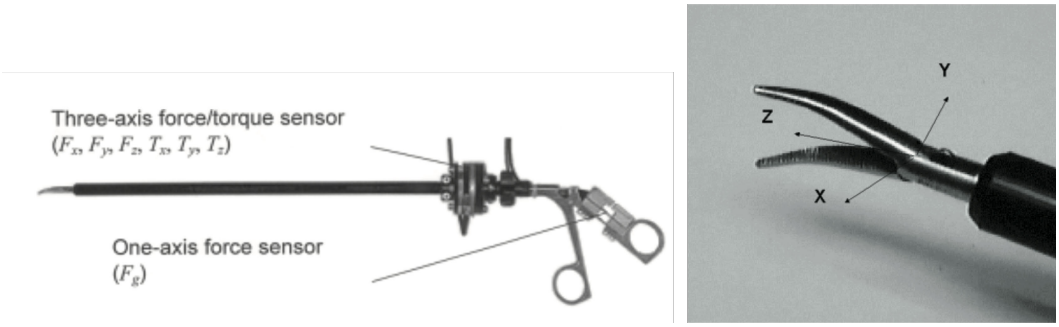

Fig. C1: laparoscopic instrument with force/torque sensor at the handle (left). Defined axes (right) [23]

Using data from Rosen et al. [23] the upper bound of the absolute force within the 95% interval of all samples in the xy-plane was calculated to be 2.9 N. The value was retrieved using ImageJ (Version 1.53e – Wayne Rasband and contributors, National Institutes of Health)

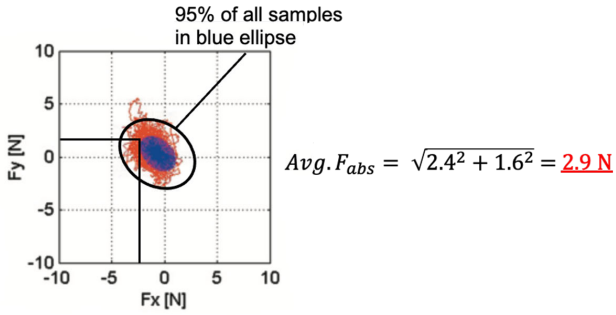

Fig. C2: Absolute force calculation based on data presented by [23]

Assuming a static scenario with the force applied 5 cm above the pivot point instead of at the handle, the force applied to the trocar could be calculated (Figure C3). Resulting in a load of 10.7 N (1.1 kg) that should be applied to the trocar.

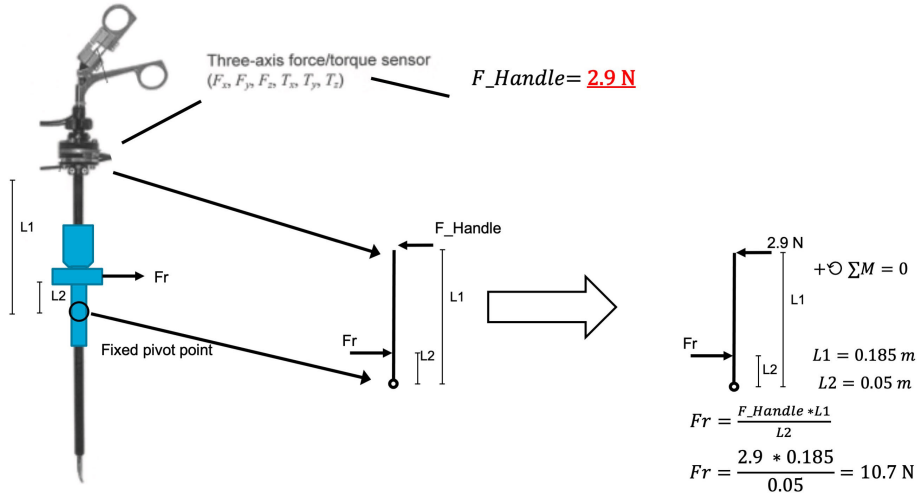

Fig. C3: Calculation of reaction force trocar

Appendix D: Flow sensor calibration

To determine the volume of CO_2 needed to saturate the acrylic container, the container was flushed (15 L/min) with CO_2, and the CO_2 concentration (volume %) was measured using a Sensirion STC31 CO_2 sensor [43]. The volume of inflated CO_2 was read from the insufflator when the container was saturated with CO_2. The procedure was repeated three times. Between measurements, the container was flushed with room air. The results of all three measurements are shown in Figure D1.

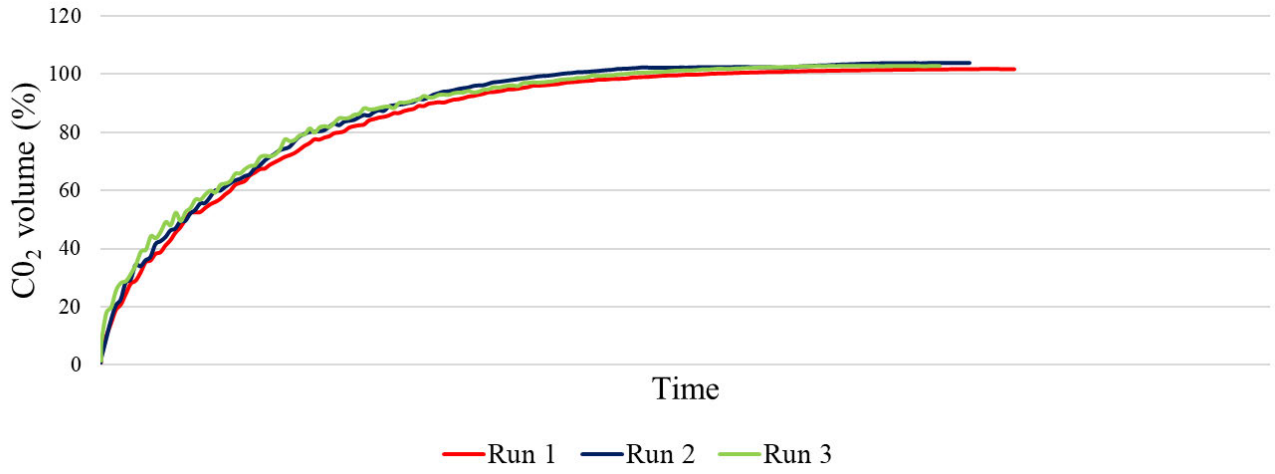

Fig. D1: CO_2 saturation over time during flushing of acrylic container.

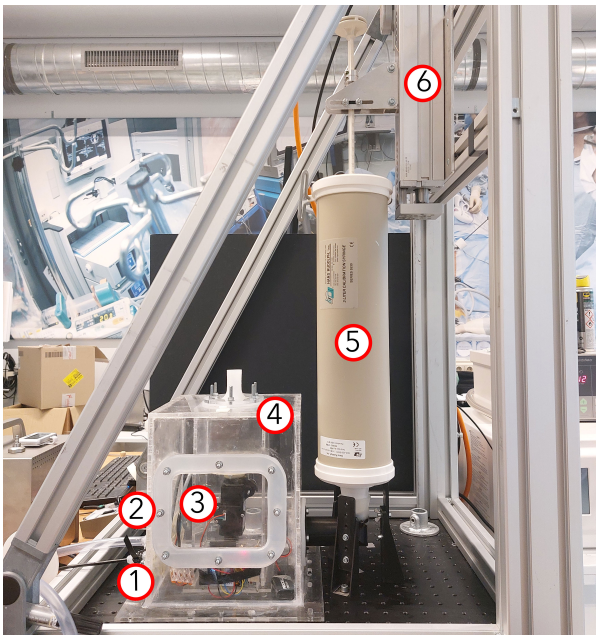

Fig. D2: Calibration Setup. 1: USB cable arduino to laptop, 2: Insufflation tube, 3: Flow sensor, 4: Acrylic container, 5: Calibration syringe, 6: Linear stage

The container was saturated with CO_2 after 32.4, 30.3, and 29.1 liters for runs 1,2, and 3, respectively. Therefore, flushing the container with 35 liters of CO_2 before testing was sufficient for proper saturation with CO_2. Before calibrating the CO_2 sensor, the container was flushed with 35 Liters of CO_2 to ensure CO_2 saturation. A three-liter calibration syringe (Hans Rudolph series 5530, Hans Rudolph inc., Shawnee, Kansas, USA) was used. The cylinder bore was 10.16 cm resulting in an area of 81 cm^2. The syringe was attached to the linear stage, and the output was connected to the container. Different flow values of (0,1,2,3,5,10,15,20,25 L/min) were programmed to the stage's controller using corresponding velocities with the bore area. The container was sealed and pressurized. Two seconds before the start of the measurement, the seal was removed, and the insufflator stopped. The preset flow was started using the linear stage controller, and flow data were recorded in Labview. The test setup is shown in Figure D2.

A total of three calibration runs were executed. The averaged results are shown in Figure D3.

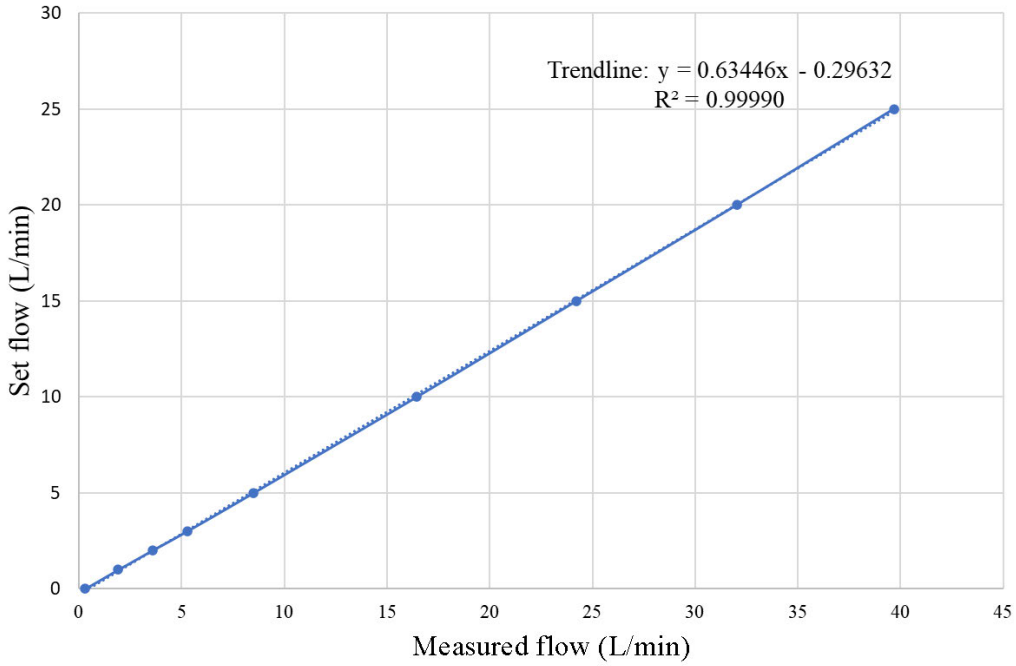

Fig. D3: Calibration curve flow sensor with linear fitting

After linear fitting to the curve, a coefficient of 0.63446 was found with a R^2 value of 0.99990. This value was used to correct the sensor output value using LabVIEW.

Appendix E: data storage LabVIEW

LabVIEW diagram

The LabVIEW diagram in Figure E1 shows the creation of a TDMS file in the bottom left corner outside the while-loop. The VISA blocks establish serial communication with the ARDUINO UNO R3. Serial data is split inside the WHILE loop in flow, pressure, and distance sensor data. Subsequently, data is processed based on previously performed calibrations. The flow offset can be set manually in the control panel. Values are displayed as numeric values and are plotted in graphs. In case the "Start measurement" control is set to TRUE, data is written to the TDMS file in a single group with a channel for all three sensor data values.

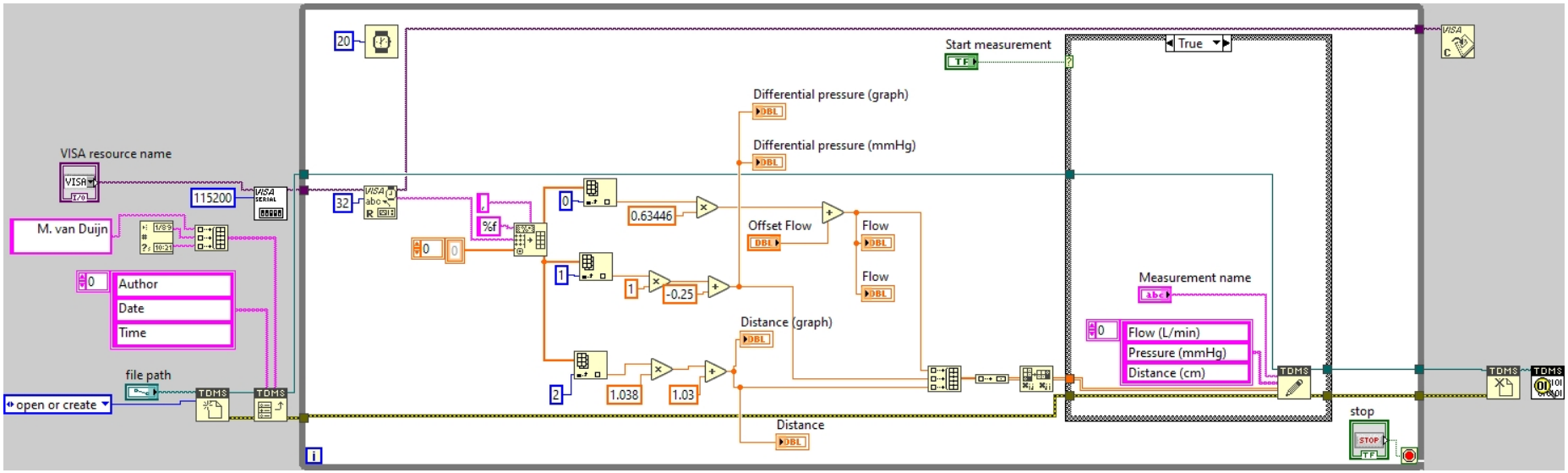

Fig. E1: LabVIEW diagram for reading, displaying, and storing sensor data.

User interface

The user interface of the LabVIEW VI (Figure E2) allows the user to choose the file path for saving the TDMS file. The VISA resource name dropdown menu allows for selecting the serial port. The Measurement name can be inserted and will correspond to the group name in the TDMS file. The ”start measurement” button starts and stops the recording of measurements. The ”Stop” button terminates the virtual instrument (VI).

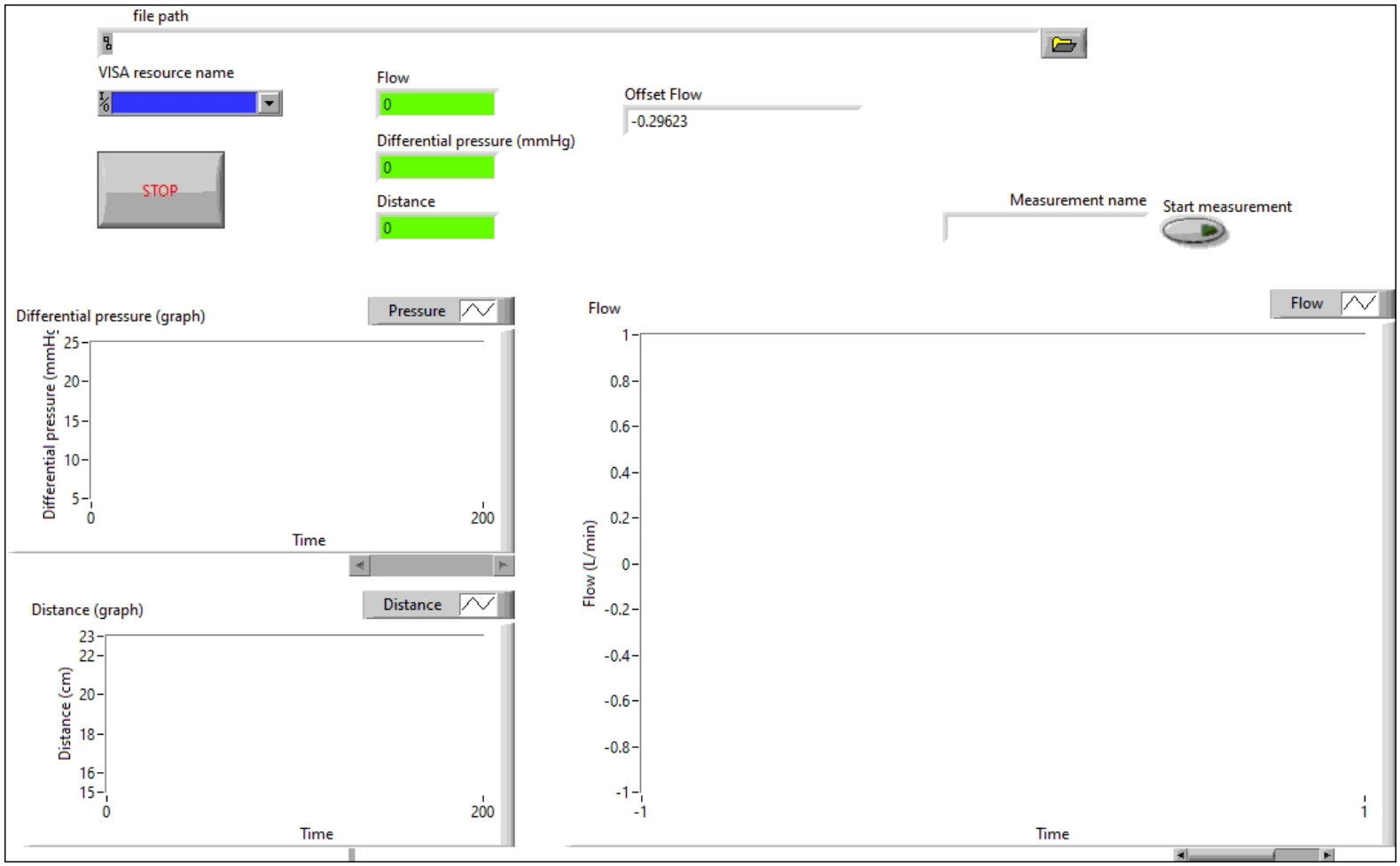

Fig. E2: User interface LabVIEW VI

Appendix F: Wiring and programming Arduino

Arduino code for CO_2 sensor with display

```
// include libraries for sensor and display
#include <Wire.h>
#include "SparkFun_STC3x_Arduino_Library.h"
#include "SparkFun_SHTC3.h"
#include <U8g2lib.h>
STC3x mySensor;
SHTC3 mySHTC3;

// configure display
 U8G2_SSD1306_64X32_1F_F_HW_I2C u8g2(U8G2_R0, /* reset=*/ U8X8_PIN_NONE);

void setup()
{
  Serial.begin(115200);
  u8g2.begin();
  Wire.begin();

  if (mySensor.begin() == false)
  {
    Serial.println(F("STC3x undetectable..."));
    while (1)
      ;
  }

  if (mySHTC3.begin() != SHTC3_Status_Nominal)
  {
    Serial.println(F("SHTC3 undetectable..."));
    while (1)
      ;
  }

  //configure sensor for CO2 in AIR with range 0-100
  if (mySensor.setBinaryGas(STC3X_BINARY_GAS_CO2_AIR_100) == false)
  {
    Serial.println(F("Gas setting could not be set..."));
    while (1)
      ;
  }

  //Compensation for temperature and humidity

  if (mySHTC3.update() != SHTC3_Status_Nominal) // Request a measurement
```

```
  {
    Serial.println(F("No data read from SHTC3 sensor"));
    while (1)
      ;
  }

  // compensate for temperature and humidity in STC31 sensor
  // read from the SHTC3 sensor
  float temperature = mySHTC3.toDegC(); // Returns temperature in degrees
  Serial.print(F("STC3x temperature is set to "));
  Serial.print(temperature, 2);
  Serial.print(F("C was "));
  // Check if temperature set fails
  if (mySensor.setTemperature(temperature) == false)
    Serial.print(F("not "));
  Serial.println(F("successful"));

  float RH = mySHTC3.toPercent(); // Returns humidity in %
  Serial.print(F("Setting STC3x RH to "));
  Serial.print(RH, 2);
  Serial.print(F("% was "));
  // Check if humidity set fails
  if (mySensor.setRelativeHumidity(RH) == false)
    Serial.print(F("not "));
  Serial.println(F("successful"));

  // Pressure is compensated by manually adding
  //absolute environmental pressure in mbar
  uint16_t pressure = 1006;
  Serial.print(F("Setting STC3x pressure to "));
  Serial.print(pressure);
  Serial.print(F("mbar was "));
  // Check if pressure set fails
  if (mySensor.setPressure(pressure) == false)
  Serial.print(F("not "));
  Serial.println(F("successful"));
}

void loop()
{
  if (mySensor.measureGasConcentration()) // Returns true value
  // if new measurement is ready
  {
    Serial.println(mySensor.getCO2(), 2);

  // display retrieved measurement on OLED display
  u8g2.clearBuffer();
  u8g2.setFont(u8g2_font_cu12_hr);
```

```
  u8g2.setCursor(16, 20);
  u8g2.print(mySensor.getCO2(), 2);
  u8g2.sendBuffer();

  }
  else
     Serial.print(F(".")); // print dots while waiting for new data

  delay(1000);
}
```

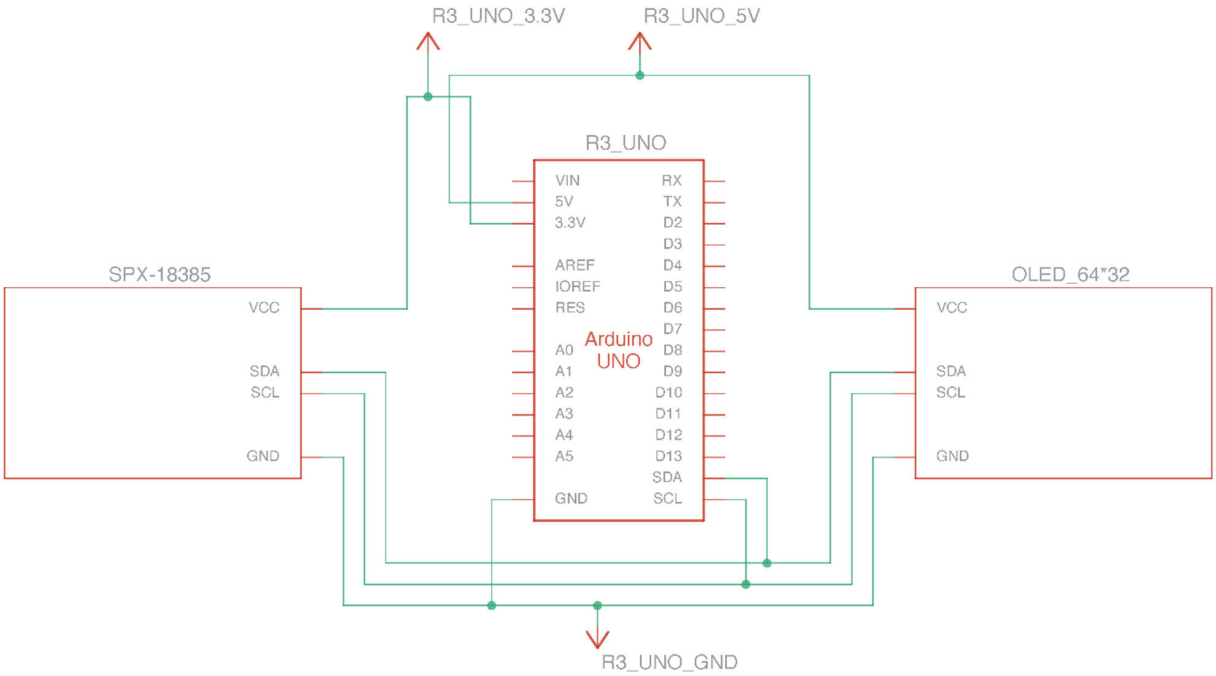

Fig. F1: Wiring CO_2 sensor with display

Arduino Code for flow, pressure and distance sensor

```
// import libraries
#include <HoneywellZephyrI2C.h>
#include <HCSR04.h>

// Distance sensor settings
float distance = 0;
//initialisation distance sensor (trigger pin = 2 , echo pin = 3)
HCSR04 hc(2, 3);

// Flow sensor settings
float SLPM = 0;
ZephyrFlowRateSensor sensor(0x49, 50, ZephyrFlowRateSensor::SLPM);

// Pressure Sensor
const int pressureInput = A3; // input pin for differential pressure sensor
const int pressureSensMax = 60; // max output of pressure sensor in mbar
float pressureValue = 0; // define value of pressure input

// Setup Communication
void setup() {
  Serial.begin(115200); // start serial communication
  Wire.begin(); // start two wire communication flow sensor
  sensor.begin(); // run sensor initialization flow sensor
}

void loop() {
// Distance sensor read
   distance = hc.dist(), 2;

// Flow sensor read
   if(sensor.readSensor() == 0) {SLPM = sensor.flow();}
   float SLPM_Cal = SLPM

// Pressure sensor read
   float pressureValue = analogRead(pressureInput);
   float voltage = pressureValue * (5.0 / 1023.0);
   float mbar = (voltage - 0.48) / 4.0 * pressureSensMax;
   float mmHg = mbar * 0.7500617;
// Displaying values
  Serial.print ( SLPM_Cal, 4 );
  Serial.print (",");
  Serial.print (mmHg, 4);
  Serial.print (",");
  Serial.println(distance, 1);
  delay(20);
}
```

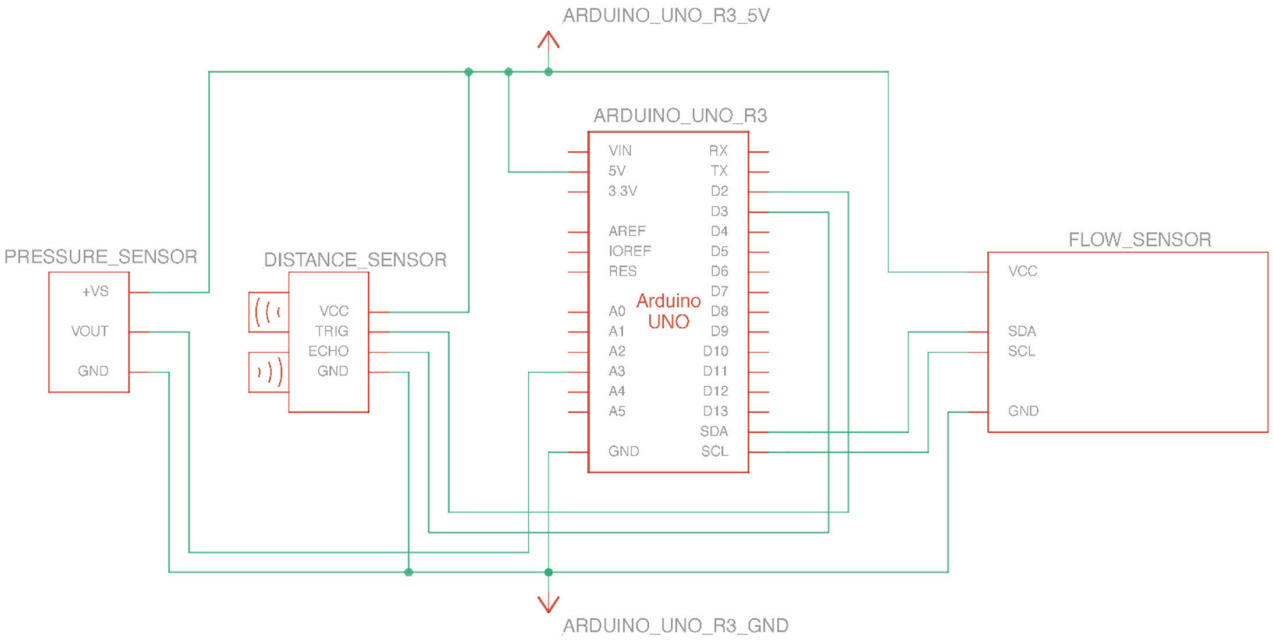

Fig. F2: Wiring Flow, pressure, and distance sensor